

**OCEAN RESOURCES INVESTIGATION  
IN THE SEA AREA OF CCOP/SOPAC  
REPORT ON THE JOINT BASIC STUDY  
FOR THE DEVELOPMENT OF RESOURCES**

**( VOLUME 3 )**

**SEA AREA OF REPUBLIC OF KIRIBATI**

**February 10, 1988**

**JAPAN INTERNATIONAL COOPERATION AGENCY  
METAL MINING AGENCY OF JAPAN**

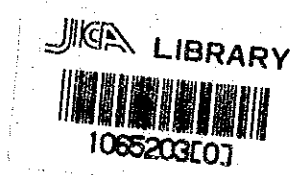
<b>MPN</b>
<b>SC</b>
<b>88-34</b>



**OCEAN RESOURCES INVESTIGATION  
IN THE SEA AREA OF CCOP/SOPAC  
REPORT ON THE JOINT BASIC STUDY  
FOR THE DEVELOPMENT OF RESOURCES**

**( VOLUME 3 )**

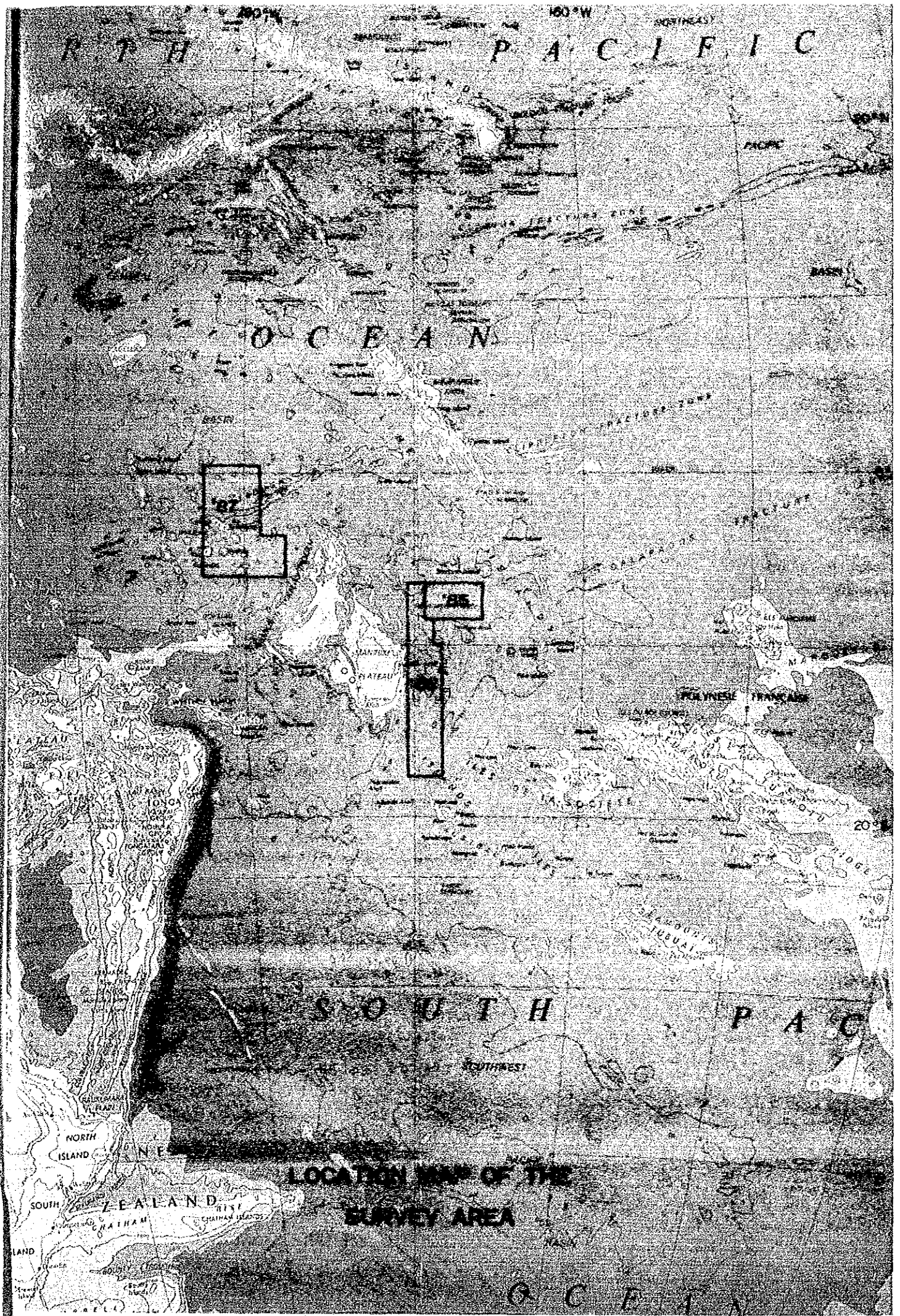
**SEA AREA OF REPUBLIC OF KIRIBATI**



**February 10, 1988**

**JAPAN INTERNATIONAL COOPERATION AGENCY  
METAL MINING AGENCY OF JAPAN**

国際協力事業団		
受入 月日	'88. 5. 6	203
登録 No.	17550	66.1 MPN



LOCATION MAP OF THE  
SURVEY AREA

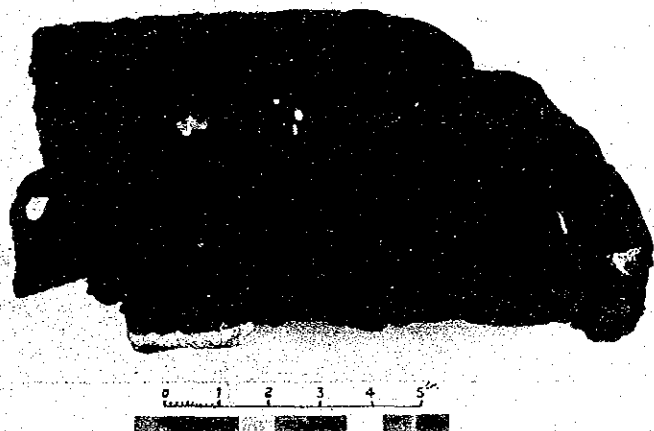




A : Cobalt crust exposure with thin foraminifera sands cover at steep slope of SA03 west seamount. Water depth: 1040m. Taken by finder attached deep sea camera.



B : Dredged samples on board. Botryoidal crust and basalt cobbles with total weight of 115kg, at SA03 west seamount. Water depth is 1,790m.



C : Section of the above(B) sample. Thickness of crust is around 5cm. Substrate is vesicular basalt with white coloured phosphate amygdules.

Representative Occurrence of Cobalt Crust in the Surveyed Area.





## PREFACE

In response to the request of the Committee for Co-ordination of Joint Prospecting for Mineral Resources in the South Pacific Offshore Areas (CCOP/SOPAC), the Government of Japan decided to conduct different studies relating to mineral prospecting such as a geological study in order to confirm the mineral resources potential on the deep ocean bottom of the offshore region of the Committee's member countries and consigned performance of the survey to the Japan International Cooperation Agency (JICA).

For the reason that essential of the above-mentioned survey belonged to the professional matters consisting of geological and mineral prospecting studies, the JICA has commissioned the Metal Mining Agency of Japan (MMAJ) to execute the survey.

The survey will be undertaken over a five year period starting from the financial year of 1985. In 1987 the third year, the MMAJ, taking the Hakurei Maru No.2, a research vessel especially commissioned for prospecting mineral resources on the deep ocean bottom, to the sites of the survey from August 29, 1987 until October 26, 1987, and finished research activities on schedule.

The present report sums up the results of the survey accomplished in the third year.

We wish to tender our sincere thanks to all the persons concerned, especially of the Secretariat of CCOP/SOPAC, the Government of the Republic of Kiribati and also of the Ministry of Foreign Affairs, the Ministry of International Trade and Industry, and the Japanese Embassies in Fiji that willingly collaborated with us.

February, 1988



---

Japan International Cooperation Agency  
President      Kensuke YANAGIYA



---

Metal Mining Agency of Japan  
President      Junichiro SATO



## ABSTRACT

We continued, this year, the survey in the adjacent area of the Republic of Kiribati on the sea areas of approximately 320,000 km<sup>2</sup> from 29th, August until 26th, October, as ocean resources investigation in the sea area of CCOP/SOPAC on the joint basic study for the development of resources in the third year. The survey was carried out for 40 days, with a view to confirm the mineral resources potential, manganese nodules, and cobalt rich crust (cobalt crust or crust in short).

The methods of the survey for the manganese nodules are as follows:

- Echo sounding prospection,
- Sampling by the sampler FG (Free Fall Grab) and SC (Spade Corer), (primary survey: 35 stations, secondary survey: 22 stations, 57 stations in total),
- Observation by CDC (60 miles in total length).

The methods of the survey for cobalt crust are as follows:

- Topographic survey on the selected five seamounts (including 2 atolls),
- Dredge sampling (48 stations),
- Observation and photographing by FDC (2 seamounts, 14 miles in total length).

As the results, the abundance of manganese nodules is not better than we expected previously, whereas that of cobalt crusts is remarkable.

The survey area can be divided in two areas whose boundary is on the Nova Canton Trough developing in the central sea area. One is the northern plain, and the other is the southern quasi-plain. General water depth is 5,200 - 5,600m. The topographic features have generally the direction of NEE-SWW trend and have much undulations with approximately 10 seamounts developing in the area. 6 among the 10 seamounts are atolls having each peak in the depth of 1,000m - 1,600m. The unconsolidated sediments are generally thin because of the above-mentioned topographic features on the sea bottom having much undulations. The unconsolidated sedimentary layer of the northern region is thicker than that of the southern region, and the maximum thickness of the stratum is about 150m. The bottom materials on the surface layer of the sediments are characterized with their prominent contrast as silicious clay of the northern region and brownish clay of the southern region.

The mode of occurrence of manganese nodules is generally discontinuous. High abundance area (> 10 kg/m<sup>2</sup>) is only in the southeastern hilly region of the survey area.

This high abundance area extends 40 miles in the E-W direction and 60 miles in the N-S direction (about 6,600 km<sup>2</sup> area). The 90% of the whole survey area has the abundance of less than 1 kg/m<sup>2</sup>. Arithmetical average of abundance of all sampling stations is 4.55 kg/m<sup>2</sup>, and weighted mean of main metal contents of all sampling stations are 0.66% Ni, 0.60% Cu, 0.22% Co, 18.74% Mn, and 13.13% Fe. Based on these average analyses, average content density of three major elements is calculated within the area having more than 20 g/m<sup>2</sup> density. The result is as follows; Ni:32.1g/m<sup>2</sup> (in 40,500 km<sup>2</sup>), Cu: 30.9 g/m<sup>2</sup> (in 34,500 km<sup>2</sup>), and Co: 40.8g/m<sup>2</sup> (in 11,700 km<sup>2</sup>). The mode of occurrence of manganese nodules of the northern half area is different from that of the southern half area. The manganese nodules of the northern area have many "r-types" with rough surface containing much Ni and Cu, while those of the southern area have many "s-types" with smooth surface containing much Co. The survey area of 5,000m - 5,200m in depth shows high abundance, while that of more than 5,400m in depth shows almost sterility. Such a mode of occurrence of the manganese nodules mentioned above has to do with the facts as follows:

- CCD (Carbonate Compensation Depth) of the survey area is around 5,200m,
- Degree of the topographic undulation is very high,
- Biological productivity variation in between the northern area and the southern area (Cronan, 1984).

As for the cobalt crust, the development of nice crusts were confirmed in almost all five seamounts except one atoll. We could find cobalt crusts on the whole survey area in the water depth from 570m to 3,400m. Maximum sampling amount could be obtained from the area in the depth of 1,600m - 2,800m, and total sampling amount was 2,770kg including substrate. The mode of occurrence and characteristics of crusts are as follows.

- a) Confirmed bearing depth of crusts is 1,000m - 3,200m, and the upper or the lower limit of the bearing depth would extend further.
- b) The mode of occurrence are crust, slab, block, cobble and nodule in shape.
- c) The inner structures of crust have various types, such as single layer, double layers, triple layers, and it generally becomes more compact in the lower layer (inner core) adjacent to the substrate.
- d) Most of the major constituent minerals is  $\delta$ -MnO<sub>2</sub>, and it often seems to subsidiarily include 10Å manganite in the inner core.
- e) The host rocks are basalt, limestone, and phosphorite.

- f) The average crust thickness among all the 32 sampled points is 1.7cm, and its maximum thickness is about 8cm.
- g) Coverage of crusts on the peaks of the seamounts is different from that on the slopes of the seamounts.  
The estimated values of coverage along the survey line of FDC will be described in this report.
- h) The average grade of samples from all the 32 sampling points are 0.78% Co, 0.66% Ni, 0.11% Cu, 25.38% Mn, and 14.48% Fe. Correlations among metal contents and correlations between each metal contents and geological factors were examined.
- i) Confirmed characteristics of crusts are almost the same as those on the seamounts distributed in the Central Pacific Ocean.

By this survey we could obtain the general informations about the occurrence of deep sea mineral resources in the survey area. We could propose the following prospection principles in the case of subsequent prospection:

- The prospection for manganese nodules should be executed mainly in the survey area having the depth range being very close to CCD value of the area and having less undulations as the topographic condition.
- The prospection for cobalt crusts could have a better potential in all the seamounts where the peak depth is less than 2,000m, and also in the middle and the lower part of atoll slopes which have comparatively small exposure on the surface (for example, Birnie Island).



## CONTENTS

	Page
Preface	
Abstract	
<b>Chapter 1. Main Points of the Survey</b>	
1.1 Title of the Survey .....	1
1-2 Sea Areas of the Survey .....	1
1-3 Objectives of the Survey .....	1
1-4 Period of the Survey .....	1
1-5 Participants in the Survey .....	3
1-6 Apparatus and Equipment for the Survey .....	4
1-7 Records of the Survey .....	5
<b>Chapter 2. Methods of the Survey</b>	
2-1 Manganese Nodules .....	7
1) Procedures of the Survey .....	7
2) Numbering of Track Lines, Sampling Stations and Sampling Points .....	7
3) Vessel Positioning .....	9
4) Sea Floor Topography .....	9
5) Superifical Sediments .....	10
6) Research on Manganese Nodules by means of MFES .....	10
7) Sampling by Means of FG & SC and Sea Bottom Observation by Means of Deep-sea Camera .....	10
8) Processing, Analyzing and Storing of Samples .....	12
9) Sea Bottom Observation by Means of CDC .....	12
10) Processing and Analyzing of the Survey Data .....	13
2-2 Cobalt Crusts .....	19
1) Procedures of the Survey .....	19
2) Numbering of Track Lines, Sampling Stations and Sampling Points .....	20
3) Vessel Positioning .....	20
4) Sea Floor Topography .....	20
5) Superifical Sediments .....	20

6) Sampling .....	20
7) Processing, Analyzing and Storing of Samples .....	21
8) Sea Bottom Observation by Means of FDC .....	21
9) Processing and Analyzing of the Survey Data .....	21
 Chapter 3. Results of the Survey · I (Manganese Nodules)	
3-1 Sea Floor Topography.....	23
1) General Topography .....	23
2) Classification of Sea Floor Topography.....	23
3-2 Superficial Sediments.....	27
1) Classification of SBP Records .....	27
2) Distribution of SBP Types .....	28
3) Thickness and its Distribution of the Upper Transparent Layer in SBP profiles .....	29
3-3 Bottom Materials .....	31
1) Classification of Bottom Materials .....	31
2) Distribution and Properties of Bottom Materials .....	31
3) Composing Minerals of Bottom Materials .....	35
4) Chemical Composition of Bottom Materials .....	35
5) Authigenic Minerals in Bottom Materials .....	39
6) CCD (Carbonate Compensation Depth).....	39
7) Identification of Microfossils in Bottom Materials .....	40
3-4 Research on Manganese Nodules by Means of MFES .....	50
1) Factors Affecting on MFES .....	50
2) Embedded Manganese Nodules .....	51
3) Estimation of Manganese Nodules by Means of MFES.....	54
3-5 Bearing Situation of Manganese Nodules .....	57
1) Classification of Types and Properties .....	57
2) Abundance and Occurrence .....	63
3) Chemical Properties .....	72
4) Mineral Properties .....	85
5) Sea Bottom Situation and Abundance .....	90
6) Observation Results by CDC .....	98
7) Distribution of Metal Quantity .....	108
3-6 Conclusions and Problems .....	110



## Chapter 4. Results of the Survey · II (Cobalt Crusts)

4-1	Seamounts Topography .....	113
	1) Classification of Seamounts and Topography .....	113
	2) Topographic Features of Seamounts .....	114
4-2	Seamount Geology .....	119
	1) General Geology of Seamounts .....	119
	2) Description of Substrates of Cobalt Crusts .....	120
4-3	Bearing Situation of Cobalt Crusts .....	132
	1) Classification of Types and Properties .....	132
	2) Distribution and Mode of Occurrence .....	142
	3) Survey Results of FDC Survey .....	146
	4) Chemical Properties .....	155
	5) Mineral Properties .....	166
4-4	Considerations.....	171
	1) Comparison among Seamounts .....	
	2) Relationship between Inner Structure of Crust and Phosphate Rock ..	

## Chapter 5. Summary

5-1	Methods of the Survey .....	175
5-2	Topography and Geology .....	176
5-3	Bearing Situation of Manganese Nodules .....	176
5-4	Bearing Situation of Cobalt Crusts .....	177
	[References] .....	183

### [Appendix]

#### List of the Survey Results

1. (Manganese Nodules (1) - (10))
2. (Cobalt Crusts (1) - (12))

#### Weather and Sea-state Data

#### Annexed Figures (1) - (18)

(List of Inserted Figures)

Figure 1-1	Location Map of the Survey Area. ....	2
Figure 2-1	Location Map of Survey Stations, Seamounts and Others .....	8
Figure 2-2	Distribution Density of Sampling Stations .....	11
Figure 2-3	Explanation on Setting Order of Three Samplers at a Sampling Station .....	12
Figure 2-4	Processing and Assaying Flowsheet of Samples (1) and (2) .....	15
Figure 2-5	Acoustic Sounding and Processing Flowsheet .....	17
Figure 2-6	Distribution of Survey Lines and Survey Stations for CDC .....	18
Figure 3-1-1	General Sea Floor Topography .....	25
Figure 3-2-1	Classification of SBP Records .....	30
Figure 3-3-1	Distribution of Bottom Materials.....	33
Figure 3-3-2	Smear Slide Photos of Bottom Sediments .....	34
Figure 3-3-3	Typical X-ray Diffraction Patterns of Bottom Sediments .....	37
Figure 3-3-4	Typical X-ray Diffraction Patterns of Authigenic Minerals .....	40
Figure 3-3-5	Species of the Typical Radiolarian Fossils (1) and (2) .....	43
Figure 3-3-6	Specise of the Typical Foraminifera Fossils .....	49
Figure 3-4-1	Distribution of Weight Coefficient .....	52
Figure 3-4-2	Relation Between MFES Intensity and Abundance of Manganese Nodules .....	53
Figure 3-4-3	Distribution of Embedded Type Manganese Nodules .....	54
Figure 3-4-4	Influence of Embedded Type Manganese Nodules on MFES Measurement .....	55
Figure 3-5-1	Morphology of Manganese Nodules (1) and (2) .....	59
Figure 3-5-2	Morphology and Sampling Weight of Mangansese Nodules .....	61
Figure 3-5-3	Size and Sampling Weight of Manganese Nodules .....	62
Figure 3-5-4	Morphology Distribution of Manganese Nodules.....	65
Figure 3-5-5	Size Distribution of Mangansese Nodules .....	66
Figure 3-5-6	Relation between Size and Morphology .....	67
Figure 3-5-7	Relation between Local Topography and Morphology .....	68
Figure 3-5-8	Relation between SBP Type and Morphology .....	68
Figure 3-5-9	Relation between Upper Transparent Layer Thickness and Morphology .....	69
Figure 3-5-10	Relation between Bottom Sediments and Morphology .....	69
Figure 3-5-11	Frequency Distribution of Five Principal Chemical Components ..	70
Figure 3-5-12	Scatter Distribution Diagram among Respective Components ..	71

Figure 3-5-13	Relation between Each Five Principal Chemical Components and Water Depth .....	76
Figure 3-5-14	Photos of Manganese Nodules for Section Analysis .....	83
Figure 3-5-15	Grade of Respective Section of Manganese Nodules (on Board Analysis).....	84
Figure 3-5-16	Photos of Manganese Nodules for X-ray Analysis .....	86
Figure 3-5-17	X-ray Diffraction Pattern of Manganese Nodules (1) and (2) .....	87
Figure 3-5-18	Macro-Photo and Microscopic Photos of Polished Thin Section of Manganese Nodules .....	89
Figure 3-5-19	Relation between Morphology and Abundance of Manganese Nodules .....	92
Figure 3-5-20	Relation between Macroscopic Topography and Abundance of Manganese Nodules .....	93
Figure 3-5-21	Relation between Microscopic Topography and Abundance of Manganese Nodules .....	95
Figure 3-5-22	Relation between SBP Type and Abundance of Manganese Nodules ..	96
Figure 3-5-23	Relation between Upper Transparent Layer Thickness and Abundance of Manganese Nodules .....	97
Figure 3-5-24	Relation between Bottom Sediment and Manganese Nodules .....	98
Figure 3-5-25	Modified Occurrence of Manganese Nodules obtained by CDC survey .....	100
Figure 3-5-26	Examples of Continuous Photos by CDC Survey .....	101
Figure 3-5-27	Examples of Photos by CDC Survey .....	103
Figure 3-5-28	Comparison between Sea Bottom Picture and Collected Samples ..	107
Figure 4-1-1	Bird's-eye View of Seamounts .....	118
Figure 4-2-1	Photos of Representative Rocks .....	127
Figure 4-2-2	Microscopic Photos of Substrates of Cobalt Crusts (1) and (2) ..	129
Figure 4-3-1	Representative Cobalt Crust Types (On Board).....	135
Figure 4-3-2	Representative Cobalt Crust Types (Section) .....	137
Figure 4-3-3	Frequency Distribution of Thickness of Cobalt Crusts.....	146
Figure 4-3-4	Modified Distribution of Cobalt Crusts along FDC-Survey Line (1) and (2) .....	149
Figure 4-3-5	Sea Bottom Pictures by FDC Survey .....	153
Figure 4-3-6	Frequency Distribution of Major Five Chemical Components.....	159
Figure 4-3-7	Correlative Diagram among Major Chemical Components (1) and (2) .....	160
Figure 4-3-8	Crust Samples used for Chemical and Mineralogical Analysis.....	163
Figure 4-3-9	X-ray Diffraction Patterns of Cobalt Crusts .....	168
Figure 4-3-10	Reflective Microscopic Photos of Cobalt Crusts .....	169
Figure 4-3-11	EPMA Figures of Cobalt Crusts .....	170

(List of Inserted Tables)

Table 1-1	Synthetic Occurrence of cobalt Crusts at Individual Seamounts ..	4
Table 1-2	List of Survey Achievements .....	5
Table 3-1-1	Classification of Sea Floor Topography .....	21
Table 3-3-1	Classification Criteria of Bottom Materials .....	31
Table 3-3-2	Sampling Ratio of Bottom Materials .....	32
Table 3-3-3	Results of X-ray Diffraction Analysis of Bottom Materials .....	36
Table 3-3-4	Chemical Composition of the Bottom Materials .....	38
Table 3-3-5	Corelations among Chemical Components of Bottom Materials ..	39
Table 3-3-6	Results of X-ray Diffraction Analysis of Authigenic Minerals ..	39
Table 3-3-7	List of Radiolarian Fossiles .....	42
Table 3-3-8	List of Foraminifera Fossiles .....	47
Table 3-5-1	Physical Properties Associated with Morphology of Manganese Nodules .....	58
Table 3-5-2	Chemical Properties of Manganese Nodules .....	72
Table 3-5-3	Morphology and Chemical Properties of Manganese Nodules .....	74
Table 3-5-4	Size and Chemical Properties of Manganese Nodules .....	77
Table 3-5-5	Sea Floor Topography and Chemical Properties of Manganese Nodules .....	78
Table 3-5-6	Bottom Sediments and Chemical Properties of Manganese Nodules	79
Table 3-5-7	Total and Minor Element Analysis of Manganese Nodules .....	81
Table 3-5-8	Chemical Compositional Difference between Outer and Inner Part of Manganese Nodules .....	82
Table 3-5-9	Result of X-ray Diffraction Analysis of Manganese Nodules .....	90
Table 3-5-10	Coverage and Abundance of Manganese Nodules at Each Station of CDC Survey .....	99
Table 3-5-11	Comparison of Abundance Obtained by FG Sampling and CDC Survey .....	106
Table 4-1-1	Classification of Topographic Type of Seamount .....	113
Table 4-1-2	Classification of Topography of Seamount .....	113
Table 4-1-3	Topographic Feature of Individual Seamount (1) and (2) .....	116
Table 4-2-1	Geology of Individual Seamount (1) • (2) and (3) .....	121
Table 4-2-2	Description of Substrates of Cobalt Crusts (1) and (2) .....	124
Table 4-2-3	Mineral Assemblage of Substrates .....	131
Table 4-2-4	Chemical Composition of Substrates .....	132
Table 4-3-1	Classification of Types of Cobalt Crusts (1) and (2) .....	133

Table 4-3-2	Occurrences of Cobalt Crusts at Individual Seamount (1) • (2) and (3) .....	139
Table 4-3-3	Bearing Rates of Different Rock Types in Each Crust Types .....	143
Table 4-3-4	Average Thickness of Cobalt Crust at Each Seamount .....	144
Table 4-3-5	Thickness Examples of Cobalt Crusts .....	145
Table 4-3-6	Average Grade of Cobalt Crusts at Each Seamount .....	155
Table 4-3-7	Cobalt Crust Grade and Topographic Position of Seamount .....	156
Table 4-3-8	Cobalt Crust Grade and Surface Structure .....	156
Table 4-3-9	Cobalt Crust Grade and Substrates .....	156
Table 4-3-10	Grade of Cobalt Crust .....	157
Table 4-3-11	Analysis of Total and Minor Element from Different Layer of Cobalt Crust .....	158
Table 4-3-12	Mutual Relations among Major Chemical Composition of Cobalt Crust .....	162
Table 4-3-13	Comparison of Cobalt Crust Compositions .....	166
Table 4-3-14	Mineral Assemblage of Cobalt Crust, by X-ray Diffraction Analysis .....	167
Table 5-1	General Occurrences of Cobalt Crusts at Individual Seamount ..	181

**(List of Annexed Figures)**

- Annexed Figure 1 Trackline Map
- Annexed Figure 2 Positions of Sampling Points
- Annexed Figure 3 Sea Floor Topography
- Annexed Figure 4 Distribution of SBP Types
- Annexed Figure 5 Acoustic Thickness of Upper Transparent Layers Obtained by SBP Survey
- Annexed Figure 6 Estimated Abundance Map of Manganese Nodules by MFES
- Annexed Figure 7 Abundance Map of Manganese Nodules
- Annexed Figure 8 Ni Grade Map of Manganese Nodules
- Annexed Figure 9 Cu Grade Map of Manganese Nodules
- Annexed Figure 10 Co Grade Map of Manganese Nodules
- Annexed Figure 11 Mn Grade Map of Manganese Nodules
- Annexed Figure 12 Fe Grade Map of Manganese Nodules
- Annexed Figure 13 Ni Metal Quantity Map
- Annexed Figure 14 Cu Metal Quantity Map
- Annexed Figure 15 Co Metal Quantity Map
- Annexed Figure 16 Trackline Maps of Individual Seamounts
- Annexed Figure 17 Topographic Plans and Sections of Individual Seamounts (1) - (4)
- Annexed Figure 18 Geology and Distribution of Cobalt Crusts of Individual Seamounts (1) - (5)

## Chapter 1. Main Points of the Survey

### 1-1 Title of the Survey

The 1987 financial year -

Joint Basic Study for the Development of Mineral Resources in the Exclusive Economic Zone of the Republic of Kiribati.

### 1-2 Sea Areas of the Survey

Pursuant to the Cooperative Study Programme and its Scope of Work relating to the deep seabottom mineral resources in the economic sea areas of CCOP/SOPAC, concluded in July 18, 1985 between the survey agency of Japan of one part and CCOP/SOPAC of the other part, the sea areas contained in a polygon (area: approximately 326,500km<sup>2</sup>, Fig. 1-1) enclosed by geodesic lines drawn between coordinates numbered in the series listed below were designated as the survey areas.

	Latitude	Longitude
1	0° 30' N	172° 30' W
2	0° 30' N	169° 00' W
3	3° 30' S	169° 00' W
4	3° 30' S	167° 30' W
5	6° 00' S	167° 30' W
6	6° 00' S	172° 30' W
1	0° 30' N	172° 30' W

### 1-3 Objectives of the Survey

The objective of the survey was to confirm the mineral resources potential on the deep sea bottom of CCOP/SOPAC sea areas.

### 1-4 Period of the Survey

Survey: August 29, 1987 - October 26, 1987

Analysis: October 27, 1987 - February 10, 1988

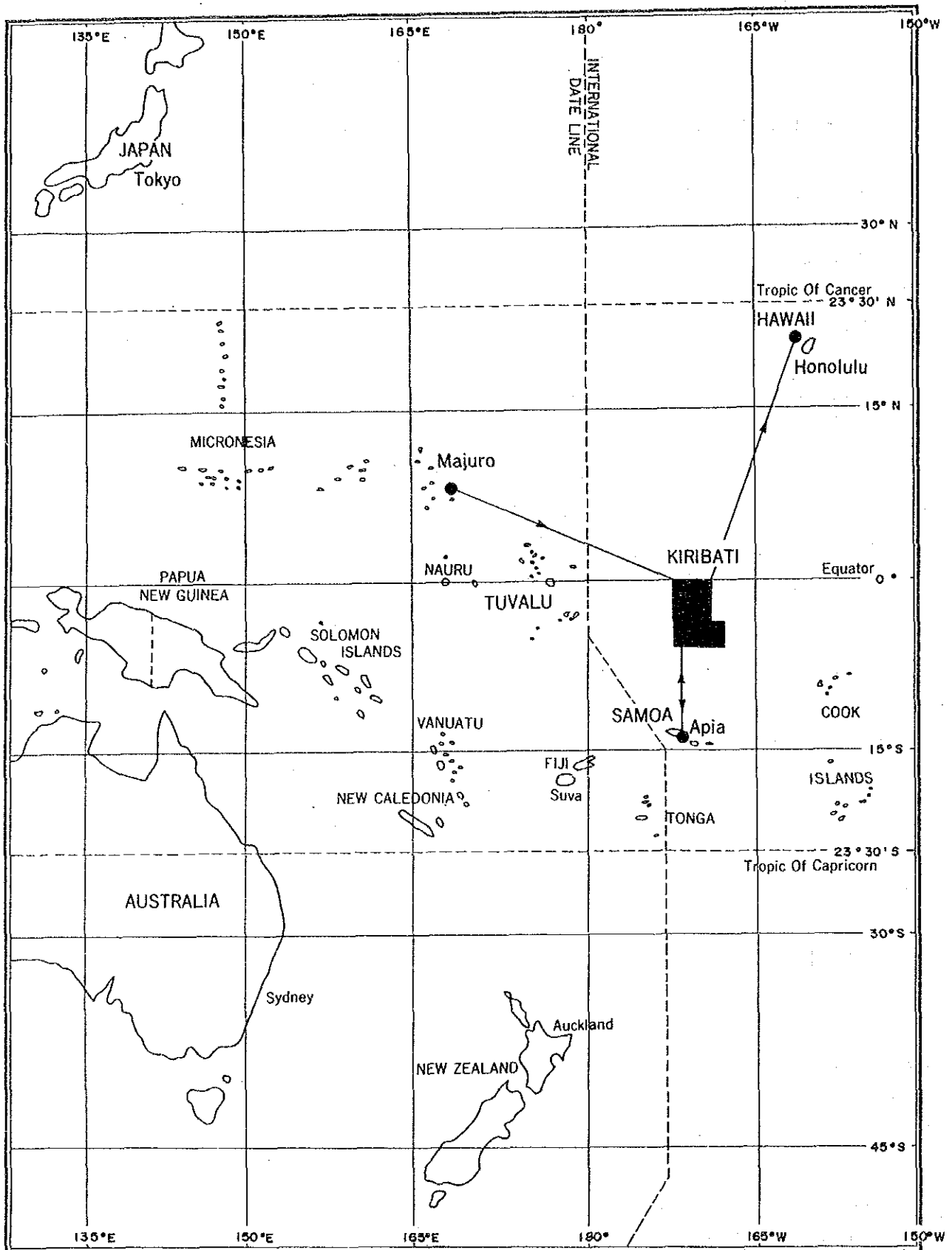


Fig. 1-1 Location Map of the Survey Area



## 1-5 Participants in the Survey

### Japanese side

#### Supervisors at the surveying sites

Motohiko KATO	(Ministry of International Trade and Industry)
Seizo NAKANO	(Geological Survey of Japan)
Toshihiko HAYASHI	(Metal Mining Agency of Japan)

#### Members of the surveying team

##### Chief of the team

Toshio TAKAHASHI	(Deep Ocean Resources Development: DORD)
------------------	--

##### Member of the team

Hiroshi KUSAKA	(idem)
Kiyoshi TONO	(idem)
Yutaka YOSHINAGA	(idem)
Kazunori MATSUI	(idem)
Hisanori TAKAHASHI	(idem)
Nadao SAITO	(idem)
Koichi HISATANI	(idem)
Yoshiharu WATANABE	(idem)
Nobuyuki MURAYAMA	(idem)
Yoshikazu YOKOYA	(idem)
Seigo KUWAHARA	(idem)
Katsuhiko EBISUI	(idem)
Susumu KAWAKAMI	(idem)
Ichiro YAMASHITA	(idem)

### Consigning side

#### Negotiators for the agreement

Jioji KOTOBALAVU	(CCOP/SOPAC)
C.A. MATOS	(idem)
C.L. TIFFIN	(idem)

#### Advisor

D.S. CRONAN	(CCOP/SOPAC)
-------------	--------------

## 1-6 Apparatus and Equipment for the Survey

The main apparatus and equipment used in the survey during the current fiscal year are shown in Table 1-1.

Table 1-1 Synthetic Occurrences of Cobalt Crusts at Individual Seamounts

	Survey method	Survey apparatus and system	Abbreviation	Remarks
Positioning		Navy Navigation Satellite System	NNSS	
Sea bottom topography and Geologic survey	Acoustic sounding	Precision depth recorder Narrow beam sounder Sub-bottom profiler Multi-frequency exploration system	PDR NBS SBP MFES	
	Sampling	Dredger  Corer Free fall grab	*1  *2 FG	*1 Chain bucket (CB) Arm-type (AD) J62 type (JD) *2 Spade corer (SC) Piston corer (PC) Gravity corer (GC)
Sea bottom observation		Deep-sea camera Continuous deep-sea camera Continuous deep-sea camera with finder	CDC  FDC	

1-7 Records of the Survey

The surveying operations were accomplished as shown in Table 1-2.

Table 1-2 List of Survey Achievements

	Item	Accomplishment
Survey schedule	Leaving Majuro Arriving in the survey area Leaving the survey area Arriving at Apia Leaving Apia Arriving in the survey area Leaving the survey area Arriving at Honolulu	Aug., 30 13:00(*) Sep., 2 02:00(**) Sep., 18 19:00(**) Sep., 20 14:00(**) Sep., 23 16:00(**) Sep., 25 04:30(**) Oct., 18 12:00(**) Oct., 24 08:00(***)
Sampling	(Manganese Nodule) Accuracy (disposition of the stations)  Sampling stations  Sampling per one station Samplers used  Failure due to non-floating	Stations at the primary stage (42.4 N miles grid) and Stations at the secondary stage (21.2 N miles grid) Primary: 35 points, Secondary: 22 points 3 samples Free fall samplers : 166 samplings Spade cores: 5 samplings none
	(Cobalt Rich Crust) Number of seamounts (including Islands) Number of dredging Amount of samples recovered	5 seamounts  48 times 2,770 kg (including rock parts)
Deep-sea camera	Use of deep-sea camera Successful cases Unsuccessful cases due to	166 times 162 times 4 times - premature flash 3 times - disorder of bottom contact switch 1 time

\* in local time at 165°E \*\* in local time at 165°W \*\*\* in local time at 150°W

	Item	Accomplishment		
		87SOD011	87SOC021	Total (average)
Sea bottom observation by CDC	Name of track line	87SOD011	87SOC021	Total (average)
	Total length of track lines	33.4	26.1	59.5 N miles
	Number of stations surveyed	18	14	32
	Required hours	29:02	20:56	49:58
	Average minutes of photographing (min/station)	8.70	9.10	(8.90)
	Numbers of photos	91	70	161
Photo analyzing	Photo analyzing	323 cases FG.SC photos 162 cases CDC photos 161 cases		
Assaying	Treatment	353 cases Ordinary samples 321 cases Manganese Nodules 196 cases Cobalt Rich Crusts 125 cases Extraordinary samples 32 cases (including 11 cases of qualitative analysis) (Ni, Cu, Co, Mn, Fe) Analyzed components Total number of analyzed components 342 cases x 5 components = 1,710 components 11 cases x (approximate 10 elements) = qualitative analysis		
Acoustic sounding	SBP 3.5 kHz	Distance of sounding survey		4,890.5 N miles
	PDR 12.0 kHz	"		4,890.5
	NBS 30.0 kHz	"		4,890.5
	M F E S	"		4,890.5
Data processing	On line MT	11 reels		
	" MIX MT	9 "		
	Sampling MT	1 "		
	" MIX MT	1 "		
	Weather·Sea state MT	1 "		
	" MIX MT	1 "		
(Total)	(24 " )			
	Name of track lines	87SFD01	87SFD02	Total (average)
	Total length of track lines (A)	9.5	3.5	14.0 N miles
	Required hours	14:40	4:37	16:17
	- setting hours	02:44*1	00:40	03:24
	- photographing (T)	07:48	02:50	10:38
	- re-collecting	01:08	01:07	02:15
	Average speed (A/T) (knot)	1.20	1.20	(1.20)
	Average minutes of photographing (min/stations)	3.20	2.60	(3.00)
	Numbers of photos	147	65	212

\*1 for 2 times

## Chapter 2. Methods of the Survey

### 2-1 Manganese Nodules

#### 1) Procedures of the Survey

The survey consisted of primary (reconnaissance) and secondary (detailed) stages. On the primary stage, the acoustic sounding and the sampling operation were carried out in order to seize the outline of the manganese nodules bearing on the deep ocean floor and select the sea area for the following stage. On the second stage, the sea bottom observation by means of CDC was executed in addition to the sampling.

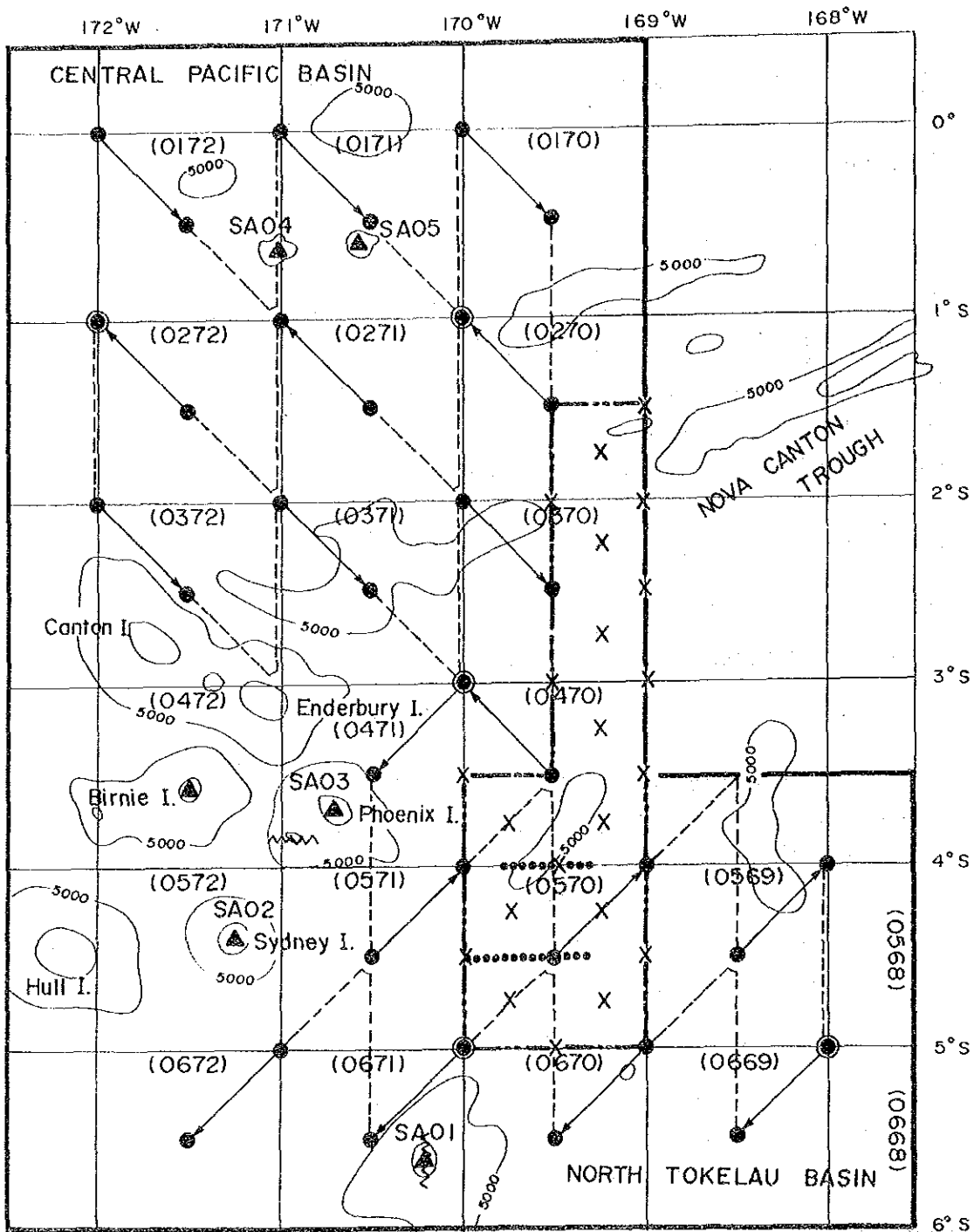
#### 2) Numbering of Track Lines, Sampling Stations and Sampling Points

##### (1) Numbering of the track lines

Numbering was put on the track lines for acoustic sounding (PDR, SBP, MBS, and MFES), so that the date and order of working were able to be identified by every cruising unit; for instance, 87S0925A, 87S0925B. For the night cruising "N" was added to the end of numbers such as 87S0925N. For the lines merely between sampling points, "P" (Position) was added such as 87S0925P. In these cases, "87S" means the financial year of the survey (1987) and the study organization (SOPAC); "0925" indicates the month of September and the date of 25th, and "A,B" the order of measuring lines on that day. The measuring lines for CDC are identified by additional numbers such as 87SCDC01, 87SCDC02 ....

##### (2) Numbering of the sampling stations and sampling points

"87S" was prefixed to indicate the financial year of the survey (1987) and the study organization (SOPAC). The surveyed sea area was divided in quadrilaterals formed with the longitudinal and latitudinal lines marked at every 1". To those quadrilaterals the area-code numbers were designated as shown in Fig. 2-1. In those numbers, the figures at the hundred digit designate south side latitudes of corresponding areas. The figures at the ten digit and the unit digit indicate west side longitudes of corresponding areas. However, these areas contain north and west sides of the numbered area and not east and south sides. The sampling carried in the areas were numbered with additional figures beginning from "01", after being marked with signs according to the respective sampling methods. From the numbering point of view, the primary survey and the secondary survey were not distinguished.



Legend

- Survey area.
  Detail survey area for manganese nodules.
- First stage sampling station,
 X Second stage sampling station for manganese nodules respectively.
- SA01 ~ SA05 : Seamounts and Islands for cobalt crust survey.
- Sampling station using spade corer.
- FDC and  CDC survey line.
- Daytime navigation,
  Nighttime navigation in the first stage survey.
- (0172): Block number.

Fig. 2-1 Location Map of Survey Stations, Seamounts and Others

Example: The sample number "87S0172FG01" signifies the first sample collected by means of FG (Free Fall Grab) in the area 0172, SOPAC in 1987.

### 3) Vessel Positioning

During the survey, all the vessel positions were indicated by "NNSS". "Corrected positions" were adopted as the vessel positions. "corrected positions" were calculated from the positions at "UP-DATE"s, which are determined by satellites, with proportional allotment according to the lapse time between "UP-DATE"s. The vessel positions as follows were registered in the field book, and it would be especially utilized for the data processing and analysis being explained later.

- 1 Starting and terminating positions on the measuring lines, course alteration points of vessel, positions at every hour of integral number;
- 2 Samplers' setting positions and their re-collecting positions;
- 3 Setting and re-collecting positions of the towing apparatus for observation by FDC, starting and terminating positions of the observation.

All the vessel positions relating to the survey activities were registered on MT with on line by using the data processing system on board. Also, the corrected vessel positions were printed out by the same system once every minute according to the respective UP-DATE in order to be utilized for compiling and analyzing the survey data.

### 4) Sea Floor Topography

As for the survey of the sea floor topography, fathoming and topographical observation were executed mainly by means of PDR between the respective stations and between the respective sampling points. Moreover, in case of FDC the observation was carried out after researching the sea floor topography in surrounding areas of the track lines as well as along the track lines. The fathoming was carried out every 12 seconds and the fathoming values indicated by PDR digitizer were registered on MT with the on-line system. In addition, every 5 minutes, water depths were recorded on the registered papers of PDR, and the sea floor topographic map was drawn with this data. The survey between the measurement stations was executed generally at the vessel speed of 10 knots, but according to the surveying situation, the vessel speed was accordingly increased or reduced. As for the track

lines between the sampling points, the vessel speed was varied around 3 - 8 knots according to the sampling operation.

5) Superficial Sediments

The survey of the superficial sediments on the sea bottom was carried out simultaneously with the sea floor topography survey, by means of SBP (frequency of 3.5 kHz) on all the cruised track lines. The basic information of the superficial sediments consists of data on the thickness of transparent layers composing the upper most stratum of the registered section pattern and on the acoustic stratigraphy type of SBP. These data were also marked in the field book every 5 minutes and used to draw the contour the Upper Transparent layer thickness map and the SBP type distribution map.

6) Research on Manganese Nodules by means of MFES

The survey on the abundance of manganese nodules was carried out by means of MFES simultaneously with the research on the sea floor topography and the superficial sediments. The measuring data produced by NBS, PDR and SBP were calculated and indicated as MFES value every 48 seconds, however it was proved that the most acceptable value of the abundance of Manganese Nodules was the moving average of 15 measured values. The measuring values of MFES were registered on MT by means of an interface with the data processing system and on the MFES floppy-discs simultaneously every 5 minutes.

7) Sampling by Means of FG & SC and Sea Bottom Observation by Means of Deep-sea Camera

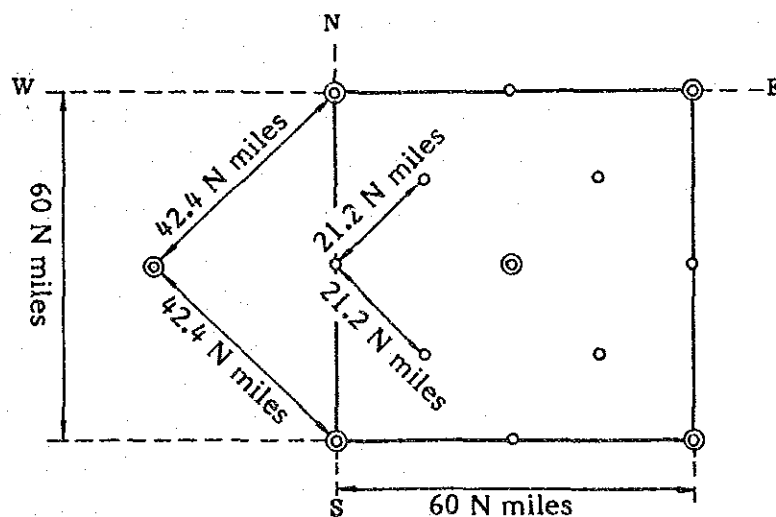
Sampling were carried out mainly by means of FG (Free Fall Grab) and partially by SC (Spade Corer). In addition to the sampling by means of FG and SC, the photographs of the sea bottom were taken by means of deep sea camera mounted on each equipment. The distribution of sampling stations for the primary and secondary surveys were chosen as follows:

- The primary stage: the sampling stations are fixed on a 42.4 N mile-grid connecting the crossing point of sectioning lines at every 1° (60 N miles) in latitude and longitude to the centre of the section.
- The secondary stage: stations covering the middle stations of the primary stage were added and the interval between the stations was reduced to a 21.2 N mile-grid.



The above-mentioned scheme is shown in Fig. 2-2. At every surveying station, three samplings were taken and the process was as follows:

The samplers set down at three apexes of the right isosceles triangle, whose centering apex located southern side of it and on the survey station. The setting down points were considered as sampling points. In other words, sampling were done just on the position of sampling station and additionally on two other points, one 1.4 N miles to the northwest and the other also 1.4 N miles northeast from the station respectively. From whichever direction the vessel approached the sampling station, it passed through the station once and after confirming the station, it returned to it and set down the first sampler. The setting order in the 3 point sampling system is illustrated in Fig. 2-3. In case of using SC instead of FG the sampler is set down, in



- ⊙ Primary survey station: 42.4 N mile grid
- Secondary survey station: 21.2 N mile grid

Notes 1) 60 N miles section correspond to every 1° in latitude and longitude

2) 1 N mile equals to 1.852 km

Fig. 2-2 Distribution Density of Sampling Stations

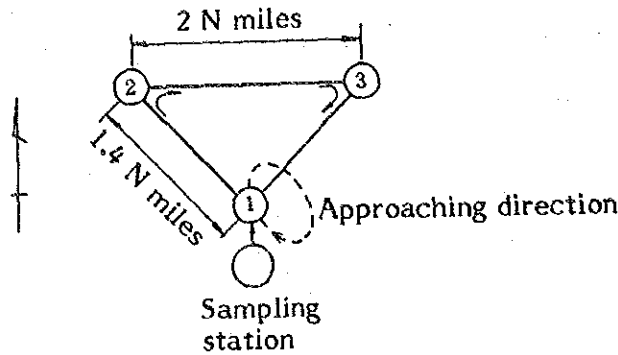


Fig. 2-3 Explanation on Setting Order of Three Samplers at a Sampling Station

principle, at the first point among the 3 sampling points. In some cases of FG sampling, it can be assumed that the sampling has been insufficient because of the FG grab troubles such as net damage and incomplete operation, which rarely happen. The grab operating accuracy (Grab Precision) was calculated by comparing the covering ratio of the manganese nodules coverage on the sea bottom photo with that on the sample collected. The grab precision is served for a reference to calculate the abundance.

#### 8) Processing, Analyzing and Storing of Samples

The re-collected samples (manganese nodules and bottom materials) were treated, on board, mainly on the basis of the processing and analyzing flowsheet of samples by FG and SC including physical measurements and X-ray analysis as shown in the Fig. 2-4 (1), (2) and (3). Some of them were also picked up for further microscopic observation, X-ray diffraction, complete analysis, micro-analysis, etc. at the laboratory and the rest were kept in storage.

#### 9) Sea Bottom Observation by Means of CDC

With a view to observe minutely the manganese nodules and sea bottom situation, the sea bottom observation by means of CDC was carried out. In selecting the observation lines for CDC, it was considered that the lines should contain the sampling stations around which the abundance of manganese nodules is higher and more continuous in the sea area of the secondary survey. (Fig. 2-6) The designed length of track lines was 60 N-miles and the interval between the observation

station was 2 N-miles. Five photographs of the sea bottom were taken for each station. The towing vessel speed was 1.0 knot during the sea bottom observation. The abundance and the average size of manganese nodules were calculated by analyzing the photos. The average of abundance and the average size of Manganese Nodules at every station were obtained by arithmetic mean of the respective values of the analyzed photos taken on the related station. In the case of the basement rock photos, its abundance value, which was assumed to be zero, was added to the number used in the calculation of the mean value of each station.

#### 10) Processing and Analyzing of the Survey Data

The processing and analyzing of the survey data were carried out mainly on board, however, a part of the data processing and synthetic analyzing were executed on shore.

##### (1) Survey data and its processing

- o The vessel positions by NNSS (date, time, latitude, longitude) were printed out in the table of rectified vessel positions every minute from the data processing system on board.
- o The depth data by PDR (NBS) (date, time, values reported from the digitizer and in the print-out papers) were registered in the field book every 5 minutes.
- o The superficial sediments by SBP (thickness of upper transparent layers, stratigraphy type) were registered in the field book every 5 minutes.
- o The values measured by MFES were registered in the field book every 5 minutes on the track lines between the sampling points and on the track lines between the observation points respectively.

The following survey data on manganese nodules, sediments, and assay etc. were registered in the field book for every sampling point.

- o Data relating to the manganese nodules: sampling amount, wet weight, wet specific gravity, morphology, number, superficial structure, etc. for each class of sized Manganese Nodules.
- o Data relating to the sediment: type of sediments, color tone, granular size, microfossil, etc.
- o Data relating to assay: grade of 5 principal components (Ni, Cu, Co, Mg, Fe) and water content.
- o Sea bottom photos by deep-sea camera equipped on FC and SC, and by CDC, re-collecting photos, working photos.

o Record photos of physical prospection (PDR records, SBP records)

(2) Analyzing of the survey data

The Map and tables essential for proceeding the survey, were drawn up using the data available on board. These data were reanalyzed afterwards on shore in further detail. The results of the analysis are shown in the following Maps and tables.

1 Map of track lines, location map of sampling points

The Map of track lines and the location map of sampling points were drawn up by plotting the position on a 1/1,200,000 scale registering sheet based on the table of recertified vessel positions printed out from the data processing system.

2 Map of sea floor topography

Using the water depth chart obtained by plotting depth values of every 5 minutes on the above-mentioned track lines chart, the map of sea floor topography was drawn with contour intervals of 200m.

3 Thickness contour map of the upper transparent layers by SBP

Thickness of the upper transparent layers was read out every 5 minutes from the SBP record and plotted on the above-mentioned chart of track lines. Then the thickness contour map was completed with contour intervals of 10m.

4 Distribution map of bottom materials

Distribution map of bottom materials was drawn by plotting types of bottom materials collected by the sampler and the quantity of authigenic minerals.

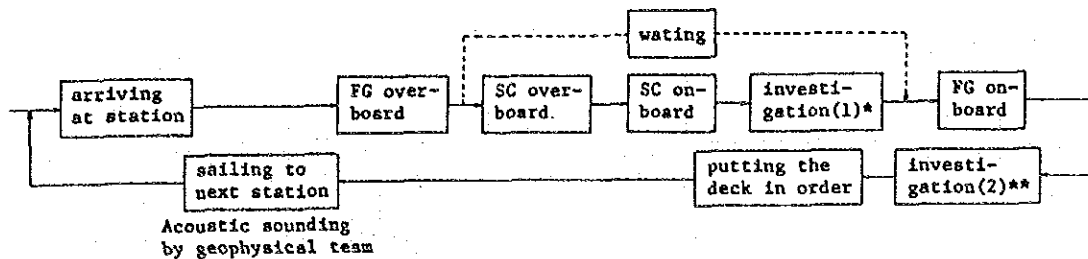
5 Abundance of manganese nodules estimated by MFES

Abundance map of manganese nodules was accomplished by plotting the abundance (MFES intensity) displayed every 5 minutes. Abundance contour lines was drawn up with the step of 25 kg/cm<sup>2</sup>.

6 Abundance map of manganese nodules, grade contour map, metal quantity map

On the basis of data obtained on the manganese nodules at each sampling point (setting down point of FG, SC, etc.), the average occurrence situation

[A] The outline of the bottom sampling work



\* Detail of investigation (1)

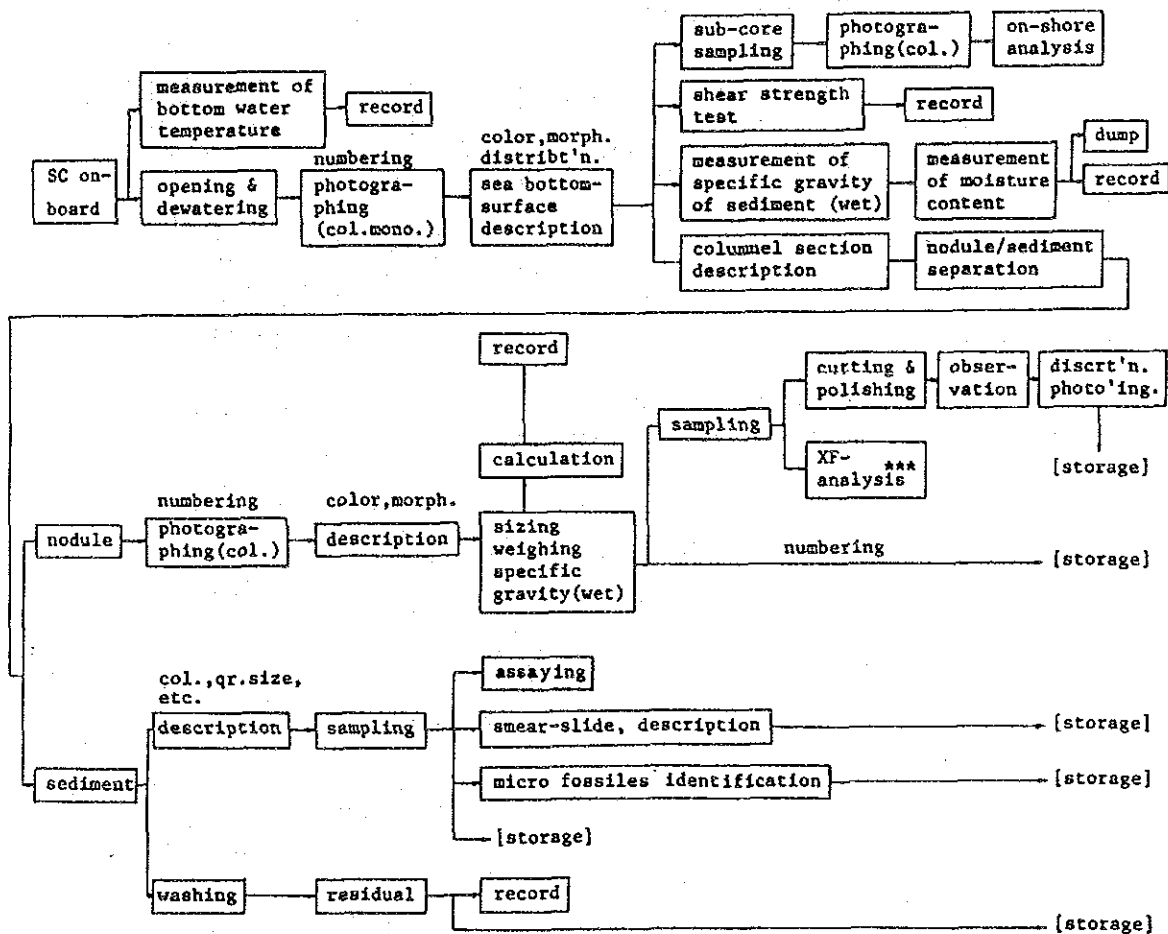
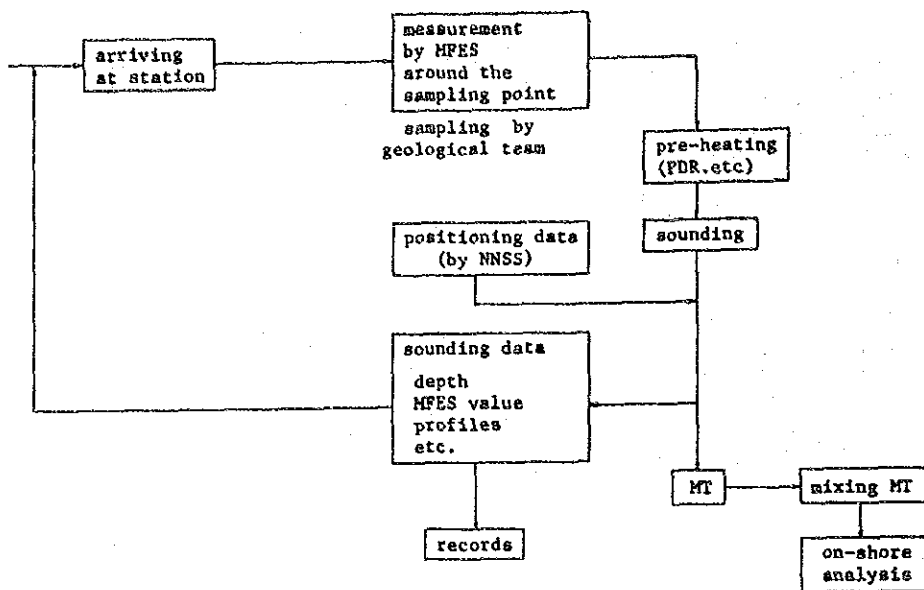


Fig. 2-4 Processing and Assaying Flowsheet of Samples (1)

[B] The outline of the acoustic sounding



After surveying, on the way to the base harbor, all data are analyzed and evaluated. The outline of them are as follows:-

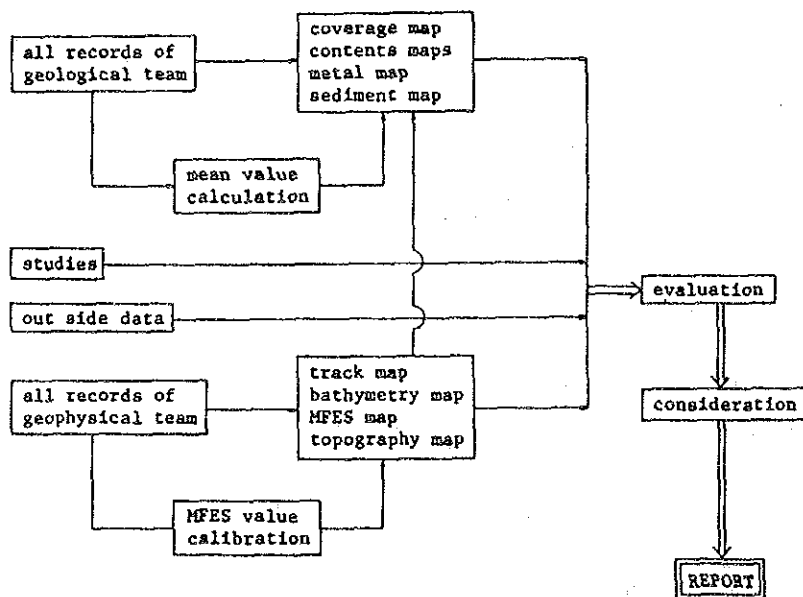
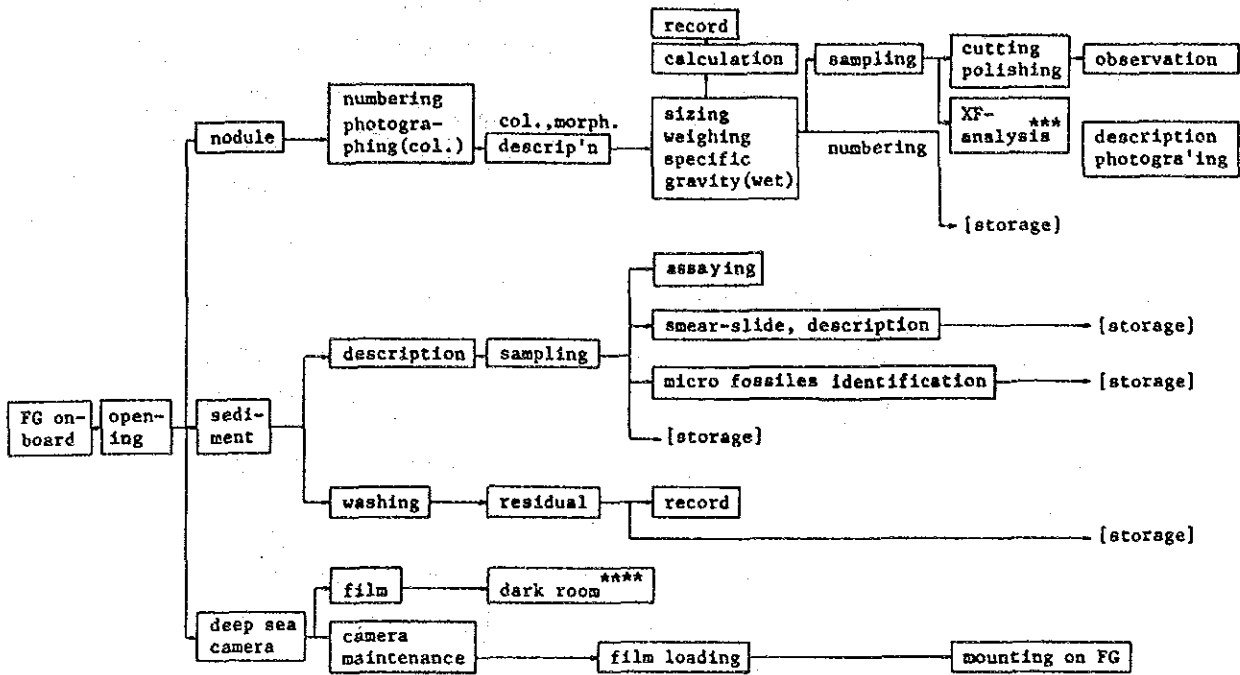
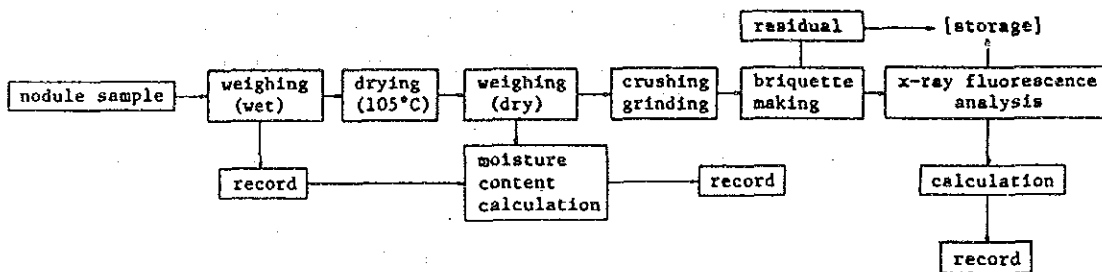


Fig. 2-4 Processing and Assaying Flowsheet of Samples (2)

\*\* Detail of investigation (2)



\*\*\* Detail of XF-analysis



\*\*\*\* Detail of dark room work

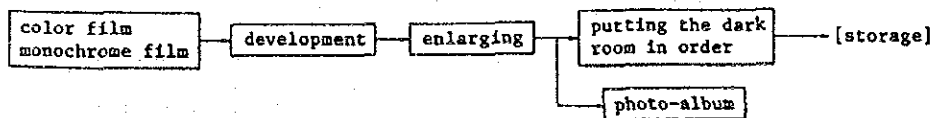
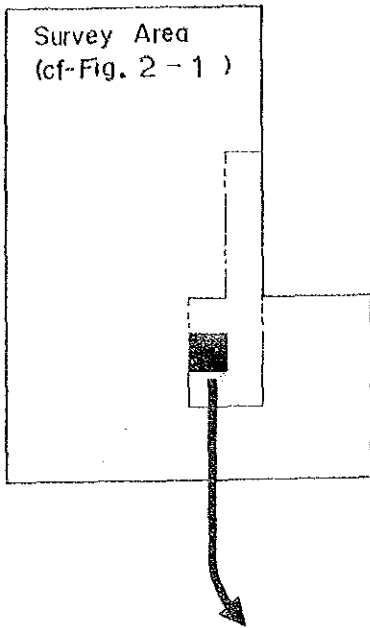


Fig. 2-5 Acoustic Sounding and Processing Flowsheet

Location Map



Legend

- Survey Sites
- Towing Direction
- Sampling Site

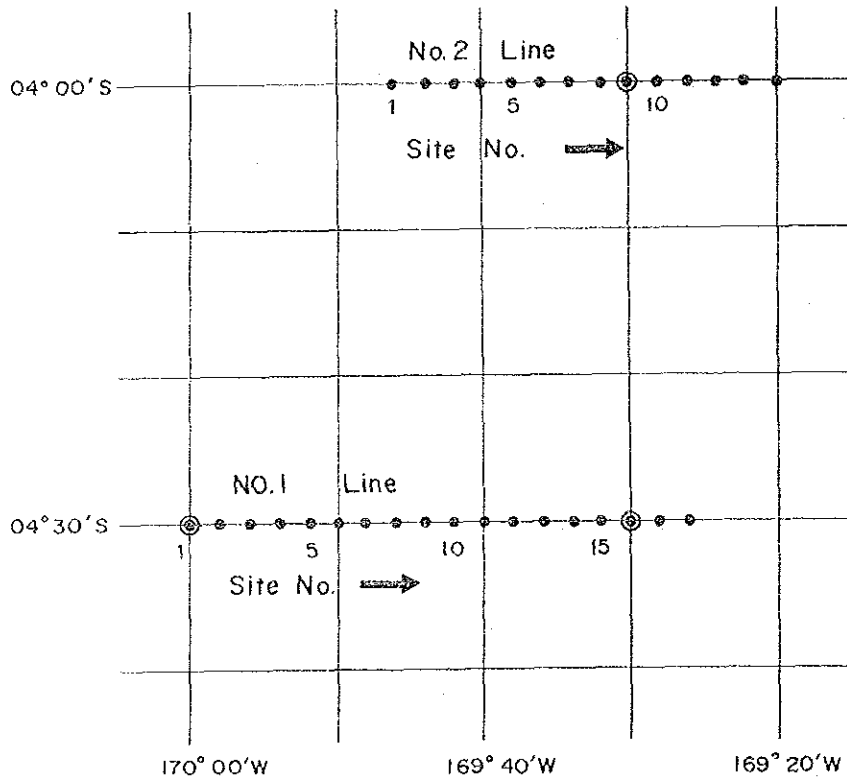


Fig. 2-6 Distribution of Survey Lines and Survey Stations for CDC



of minerals (values of abundance and grade etc.) was obtained for each station (3 samplings per one station). On the basis of these results, the abundance of manganese nodules, the grade contour map of nickel, copper, cobalt, manganese and iron and the metal quantity map of nickel, copper, and cobalt are drawn. The acoustic sounding data were also utilized in this process.

#### 7 Table of the survey results

In order to facilitate searching and consulting of the data on the manganese nodules obtained every day on board, the essential items\*<sup>1</sup> were captured in the table from the field book.

#### 8 Estimated abundance map by CDC photo

Estimated abundance by CDC photo was calculated from coverage of manganese nodules on the CDC photos using the empirical formula introduced by analyzing FG sampling data statistically. Based on these data, the estimated abundance map by CDC was accomplished.

#### 9 Analyzing the other relation between each of the elements such as abundance, grade, morphology, bearing situation, of the manganese nodules, topography, upper transparent layers' thickness, etc., studies have been carried out to define the potential field of manganese nodules.

### 2-2 Cobalt Crusts

#### 1) Procedures of the Survey

Five seamounts were selected on board for survey, based on the sea floor topographical data which had been already known and obtained from the primary survey of manganese nodules. (Fig. 2-1) These five seamounts include two islands (Sydney Is. and Phoenix Is.). The survey mainly consisted of getting the seamount topography and superficial sediments by means of the acoustic sounding and of sampling by means of dredge. Partially, the sea bottom observation and photographing were practiced.

---

\*1 The principal items are as follows:

latitude, longitude, water depth, granular size distribution, abundance, morphology, grade, sediment, state of combinations, etc..

## 2) Numbering of Track Lines, Sampling Stations and Sampling Points

Numbering of the seamounts was put on as follows.

(Seamounts) SOPAC(S)-KIRIBATI (A... begin with A, apply BC... successively for other sea areas from the next year)-No.

Example: SA01.

(Sampling points)

year-seamounts-type of dredges-No.

Example: 87SA01AD01

(Measuring lines for FDC)

year-SOPAC(S)-FDC-No.

Example: 87SFDC01

(Track lines for acoustic sounding)

year-SOPAC(S)-date-N(night)

Example: 87S0901N

(Apparatus and Equipment used in the Survey)

These are shown in Table 1-1.

## 3) Vessel Positioning

The vessel positioning was the same as that for manganese nodules. The vessel positioning for FDC was also the same as that for CDC in manganese nodules.

## 4) Sea Floor Topography

The sea floor topography was obtained by means of NBS and PDR etc. The sea floor topographic map was drawn with a plotter. The designed distances between the track lines were 4 miles as a standard and 2 miles if necessary. The vessel speed was normally 10 knots.

## 5) Superficial Sediments

The bearing situation of superficial sediment of the seamount was obtained by means of SBP. That was helpful for us to selecting the sampling points.

## 6) Sampling

Sampling were carried out by means of dredges on all five seamounts. Many types of dredges were used for various purposes. (Table 1-2) Sampling areas contained

the top and slope of the seamount within less than 3,500m in depth. The sum of samples on each seamount was approximately 10. The vessel speed was 0.5 - 1.5 knot at the time of dredges. The standard towing time between the dredge's on and off bottom is approximately 30 minutes.

#### 7) Processing, Analyzing and Storing of Samples

The dredged samples were weighed and registered in characteristics after being classified into several types on board. The part of every sample was analyzed into its five component parts such as Co, Ni, Cu, Mn, Fe, and the water content. Analyzing methods were the same as those of manganese nodules; however, the tests for deviations of data (the bias tests) were examined with the same samples which were taken to the laboratory. Microscopic observation, X-ray diffraction, total analysis, micro-analysis, etc. were carried out at the laboratory in the same way as manganese nodules. Some typical samples among the rest of the examined samples were stored with water-sealed in plastic bottles, and the rest were stored with dry in wooden boxes.

#### 8) Sea Bottom Observation by Means of FDC

In order to observe the bearing situation of cobalt crusts and take photographs of the typical situations, the survey by FDC was practiced on the tops of the two seamounts. The designed length of track lines was 10 miles and 5 miles, and the standard vessel speed was 1.0 knot during the observation. In principle, the photos were taken continuously along the sea bottom. Interval times between the shots were not fixed. A TV camera for finder was loaded on the FDC vehicle, so that the real time observation on seabottom was carried out and that detail and detective observation was repeated afterwards by VTR. The bearing situation of cobalt crusts, especially the covering ratio of crusts and the lateral variation of crust types, which could not be obtained from the sampling, were able to be analyzed by the VTR and photographs.

#### 9) Processing and Analyzing of the Survey Data

##### (1) Survey data and its processing

These were basically the same as in the case of manganese nodules. However, measuring by MFES was not practiced in the cobalt crust survey. And FDC was used instead of FG, SC and CDC.

(2) Analyzing of the survey data

The results of the on board and on shore analysis are shown in the following charts and tables.

1 Map of track lines

The Map of track lines was drawn on a 1/300,000 scale for each sea mount.

2 Map of sea floor topography, location map of sampling points

The map of sea floor topography was drawn on a 1/300,000 scale by means of X-Y plotter, and the sampling points (approximate position) were shown in there.

3 Cross section of sea floor topography

Based on the data of 2, the cross section of sea floor topography was drawn by means of X-Y plotter.

4 Geological map of sea floor and abundance map of cobalt crusts

The map was completed for every seamounts with showing the sampling data by dredges and observation data by FDC on the map of sea floor topography. The average grade of each sampling was also shown in the map.

5 Estimated abundance Map by FDC observation

The bearing situation of cobalt crusts obtained from VTR and photo analysis, the track lines of FDC, the cross section of sea floor topography, the estimated coverage ratio of cobalt crusts, etc were shown as a route map.

6 Analytic Map of characteristic factors were drawn, and studies have been carried out to define the potential field of cobalt crusts.

## Chapter 3. Results of the Survey · I (Manganese Nodules)

### 3-1 Sea Floor Topography

#### 1) General Topography

The explanations of sea floor topography of the whole surveyed area are shown in Fig. 3-1-1 and Annexed Fig. 3. The mountainous area spreads in the central part of the surveyed area and separates the surveyed area into the northern part showing the plain and the southeastern part the quasi-plain. "NOVA-CANTON trough" extends from the eastern edge of the area to east-northeast. The plain, in the northern part of the surveyed area, develops between 5,200 - 5,600m (average: 5,400m) in water depth except the seamounts. Several knolls (approximately 5,000m in depth) and troughs (approximately 5,800m, up to 6,000m in depth), were observed. The existence of two seamounts above 3,500m in relative height was newly confirmed. (SA04 Seamount: top depth 1,040m, SA05 Seamount: top depth 1,170m) The quasi-plain, in the south-eastern part of the surveyed area, spreads between 5,400m - 5,600m (average: 5,500m) in water depth and has typical undulation spreading from north-west to south-east. Generally, the undulations are larger than those in the northern plain. In this province, the existence of three seamounts over 2,500m in relative height was confirmed. (SA01 seamount: top depth 1,900m, otherseamounts: top depth 2,960m, and 3,570m) The mountainous area in the central part consists of two groups of seamounts; one is Phoenix islands which have been considered as disposed from north-west to south-east direction (for example, Canton-Enderbury-Phoenix and seamounts distributed parallelly with that), and the other is the lines of seamounts which are disposed in east-northeast direction along Nova Canton Trough and cross Phoenix Islands. The seamounts are classified into atoll, peaked seamount, compound seamount, etc.

#### 2) Classification of Sea Floor Topography

To describe the bearing situation of manganese nodules, the sea floor topography was divided macroscopically and microscopically. Definitions of topographical classification are shown in Table 3-1-1. The sea floor topography of the present surveyed area can be divided macroscopically into 3 provinces, which are the plain in the northern part (northern part of 2° 00' S), the mountainous spreading in approximately east-west trend in the central part and the quasi-plain in the

southeastern part (the eastern part of 170° 30' W and the southern part of 2° 30' S)  
 These macroscopically devided topographic provinces are called as below. (Fig. 3-1-1)

- 1 the plain to the southern edge; "Central Pacific Basin"
- 2 the mountainous; the part of "Nova Canton Trough"
- 3 the quasi-plain; the northern edge of "North Tokelau Basin".

Table 3-3-1 Classification of Sea Floor Topography

Topographical classification		Definition
Regional province	Plain	Area whose bottom is almost flat and even with a isolated sea mount or sea knoll, it may be considered as plain from a general point of view;
	Hilly	Area where numerous sea hills or sea mounts are dispersed;
	Mountainous	Area where a group of sea mounts are located;
	Quasi- plain	Area where the outstanding mounts or hills are scarcely observed but the bottom is rather undulated and which is classified neither as plain nor as hilly.
Local area	Flat	Plain area not undulated or smoothly undulated (up to about 100 m relative height) and which doesn't belong to neither the hollow nor the platform.
	Hollow	Area with smooth undulation and which presents a generally concave terrain, including a ship- shaped basin.
	Channel	Long and narrow concave terrain in a ditch shape, including fissures or fracture zones.
	Platform	Area with smooth undulation which presents as a whole a convex terrain (or a tableland)
	Sea Knoll	Hilly area with a relative height of more than about 1,000 m, including entire slop as well as summit
	Sea mount	Hilly area with a relative height of less than about 1,000 m, including entire slop as well as summit (the sloping surface contains a shifting part of the plain)
	Ridge	Terrain presenting a chain of mountain composed of the sea knolls and hills ranged in a zone.
	Other	Terrain not belonging to any of the above-mentioned classifications.

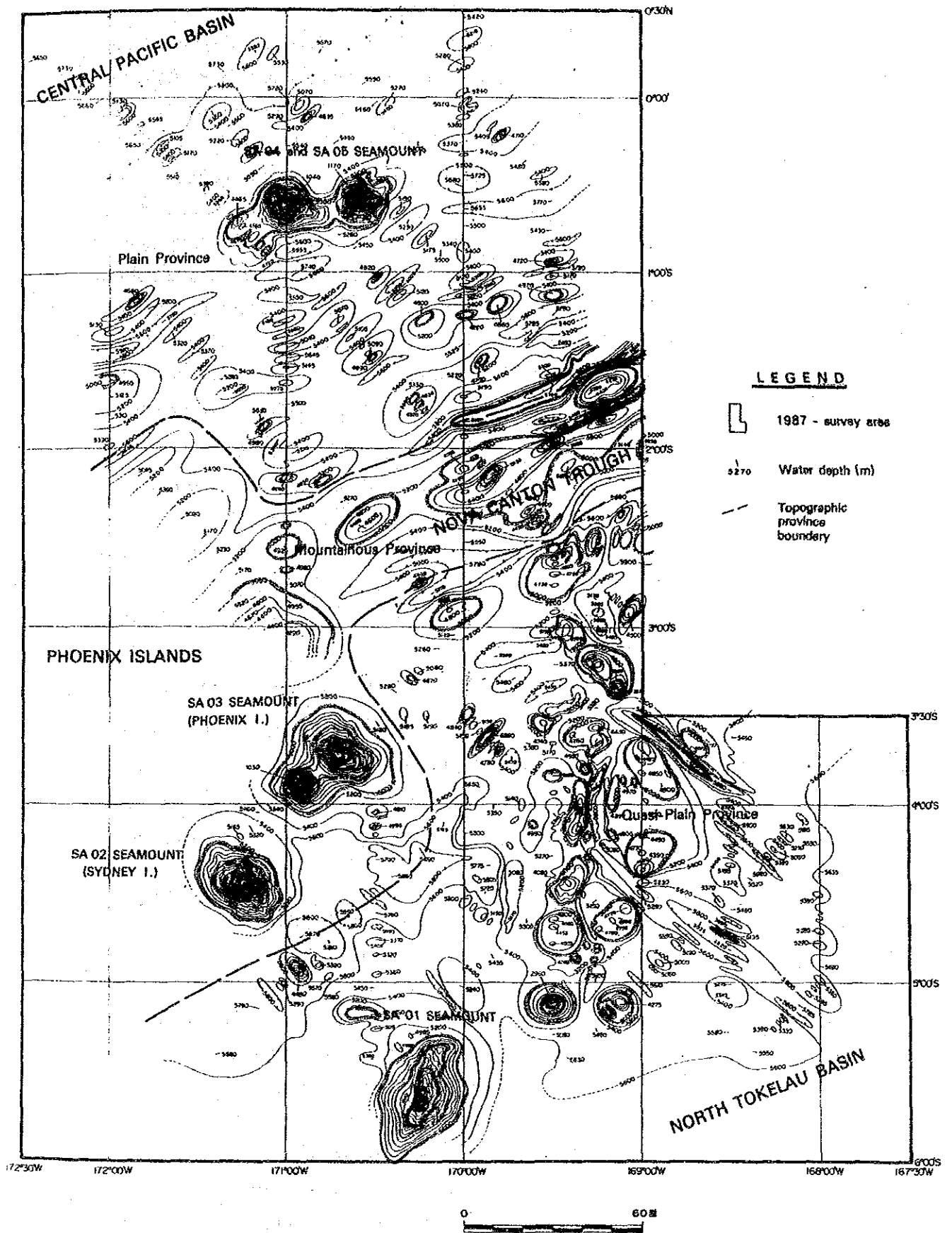


Fig. 3-1-1 General Sea Floor Topography





On the outskirts of the mountainous, troughs more than 6,000m in water depth spread parallelly with them. The sea floor topography of the present surveyed area can be divided microscopically into flats, hollows, channels, platforms, knolls, seamounts, etc. Flats spread widely over the northern part and southeastern part. Hollows are distributed spottedly in a small scale over the northern plain and slightly observed in the boundary between the southeastern quasi-plain and the mountainous. Channels spread both on the outskirts of the eastern mountains and around the knolls in the southeastern part of the surveyed area. Platforms are not observed remarkably, but slightly distributed spottedly over the northern part and the south-eastern part. Sea knolls are distributed in the south-eastern quasi-plain. It should be noticed that sea knolls are disposed in the north-south direction and cross Nova Canton Trough. Their relative heights are around 920 - 580m.

Typical seamounts are SA01 seamount, SA02 seamount (atoll), SA03 seamount (atoll), SA04 seamount and SA05 seamount: SA04 and SA05 were newly discovered in this survey. The existence of the other 3 seamounts above 1,000m in relative height were confirmed.

### 3-2 Superficial Sediment

#### 1) Classification of SBP Records

SBP records are classified into 8 types: type a, type b, type bc, type c, type d, type d<sub>2</sub>, type ds and type e, based on their reflective patterns in the surveyed area. (Fig. 3-2-1). Definitions and characteristics of each type are as follows:

##### 1 Type for which the acoustic transparent layers are recognized

Type a: presenting a double layer structure of transparent and opaque, the transparency of the transparent layer is high (faded out completely) and the boundary with the opaque layer is relatively clear; the thickness of the transparent layer measures 10 -50m.

Type b: similar to type a, composed of two layers such as transparent and opaque, but the transparency of transparent layer is not so high as to be called completely transparent.

The thickness of transparent layers measures 30 - 100m and generally the thickness is more than 50m; however, in the surveyed area, the thickness is almost less than 50m. The thickness varies markedly as compared to other type.

Type e<sub>1</sub>: presenting the multistratified structure of transparent and opaque layers; the clear stripe thin opaque layer is recognized directly beneath the upper transparent layer. The thickness of the transparent layer including that of the striped opaque layer is generally 10 - 40m.

The distribution area of these transparent layers nearly corresponds to that of brown clay and siliceous clay.

## 2 Types for which the acoustic transparent layers are not recognized

Type d<sub>1</sub>: composed only of opaque layers. Generally, this type is found at seamounts, knolls, etc., and these sites correspond approximately to their exposed basement rocks.

Type d<sub>2</sub>: similar to type d<sub>1</sub>. It is composed only of opaque layer, and this type is observed mainly in plains and these sites correspond approximately to basement rocks or coarser grained sediments.

## 3 Other types (Fig. 3-2-1)

Type ds: it may be composed only of opaque layers; for this type, the records are not clear because of the dispersion of sounding waves by the undulated floor.

Type bc: basically, it may be composed of double layers: transparent and opaque, similar to type b; the bottom surface of the top superficial layer indicating a transparent layer does not form one line but always contains some noise, and further the transparency is unstable and partially presents the opaque layer.

## 2) Distribution of SBP Types (Annexed Fig. 4)

The surveyed area consists of the plain in the northern part, the mountainous in the central part and the quasi-plain in the southeastern part. In the SBP records, the types having transparent layer are mainly observed in the plain, and the types not having transparent layer become predominant ones in the mountainous. Both types are observed equally in the quasi-plain.

### 1 Plain (northern part of the surveyed area)

This part is classified into a plain province, where type b is distributed almost in the whole area. Type d<sub>1</sub> and d<sub>2</sub> are observed on the two sea mounts, topographic height and channels, while type bc is distributed in the flat sea floor of the

northern part of  $00^{\circ}$  and the water depth is more than 5,600m. The thickness of the upper transparent layer in type b is relatively thin and approximately 10 - 50m, while that in type bc is thick and approximately 100 - 150m.

## 2 Mountainous (central part of the surveyed area)

In this area, type  $d_1$  is distributed along NOVA CANTON TROUGH. Type  $d_2$ , type ds and type b are observed in the channels. Type  $d_2$  is distributed in rather flat sea floor of the western part, while type b is distributed in the eastern side of the two seamounts. The upper transparent layer in type b has 10 - 50m in thickness.

## 3 Quasi-plain (southeastern part of the surveyed area)

Type  $d_2$  is distributed around the seamounts knolls and channels lying in a north-south row. Type  $d_1$ , type ds, type a and type b are observed on the seamounts, sea knolls and channels, so that every types are distributed intricately corresponding to the undulating topography. In the flat sea floor of the eastern part of  $170^{\circ}$  W, type b is widely extended, and type  $d_1$  is distributed partially in the topographic height.

## 3) Thickness and its Distribution of the Upper Transparent Layer in SBP Profiles (Annexed figure 5)

The distributional situation of the upper transparent layer is nearly corresponding to that of the types of the SBP record. Observing the thickness of the upper transparent layer by respective SBP type, for type a, thickness measures 10 - 50m; for type b, 10 - 50m, for type bc, 100 - 150m; for type  $e_1$ , 5 - 30m; while for type c,  $d_1$ ,  $d_2$  and ds, transparent layer was not recognized.

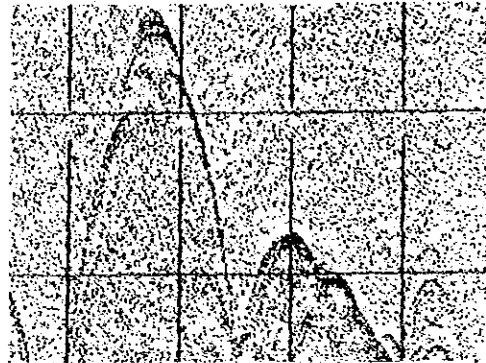
Type a

Line No. 87S0907N  
1°02'S • 172°00'W



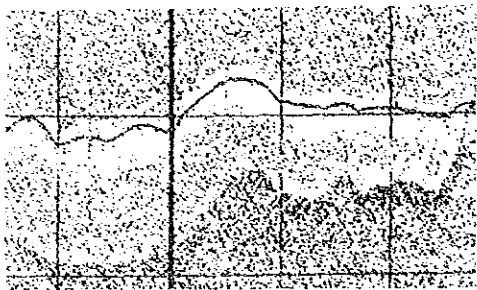
Type d<sub>1</sub>

Line No. 87S0906A  
1°18'S • 170°42'W



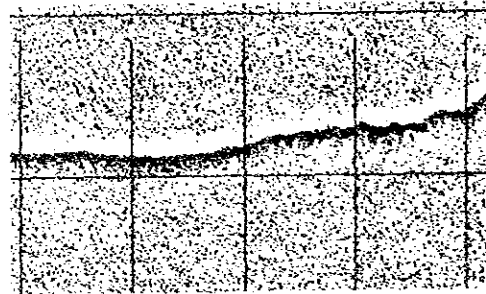
Type b

Line No. 87S0904A  
0°04'S • 169°57'W



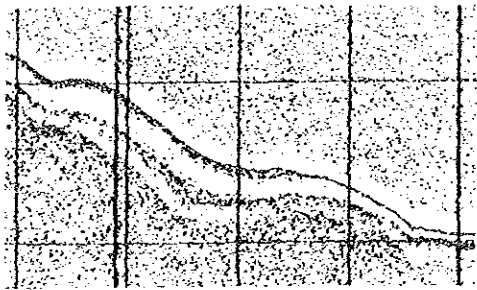
Type d<sub>2</sub>

Line No. 87S0908N  
2°32'S • 171°25'W



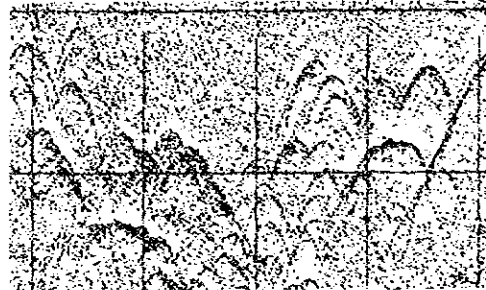
Type e<sub>1</sub>

Line No. 87S0916N  
5°30'S • 169°30'W



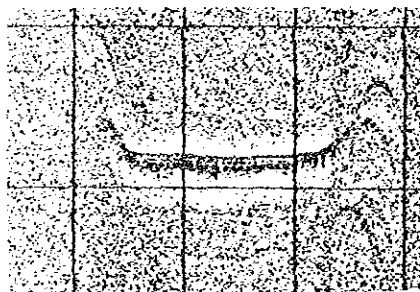
Type ds

Line No. 87S0910N  
2°52'S • 169°30'W



Type c

Line No. 87S0913N  
3°45'S • 168°48'W



Type bc

Line No. 87S0901N  
0°23'S • 172°48'W



Fig. 3-2-1 Classification of SBP Records

### 3-3 Bottom Materials

#### 1) Classification of Bottom Materials

Classification of bottom materials is done according to the classification criteria of bottom materials as shown in Tab. 3-3-1. Quantitative analysis of each composition was made by the microscope observation using Smear slide (x100).

Table 3-3-1 Classification Criteria of Bottom Materials

	Total Fossil (%)	Siliceous Fossil (%)	Calcareous(*1) Fossil (%)	Remarks(*2)
Brown clay	< 10			
Siliceous clay	10 - 30		< 5	
Silic-calcareous clay	10 - 30		>5	Siliceous fossil > Calcareous fossil
Calc-siliceous clay	10 - 30	> 5		Calcareous fossil > Siliceous fossil
Calcareous clay	10 - 30	< 5		
Foraminifera woods	> 30			Mainly foraminifera dominant
Silic-calcareous woods	> 30		5	
Siliceous woods	> 30		5	

\*1 Radiolaria, Diatom, Silicoflagellate, Sponge spicule

\*2 Foraminifera, Calcareous nanoplankton.

#### 2) Distribution and Properties of Bottom Materials

##### 1 Distribution

The sampling ratio of bottom materials is shown in Tab. 3-3-2, and the distribution of bottom materials is shown in Fig. 3-3-1. Bottom materials in the surveyed area are mainly composed of brown clay, siliceous clay and calcareous clay. Brown clay are mainly distributed in the southern part of 3° 00' S, while siliceous clay are mostly observed in the northern part of 3° 00' S.

Table 3-3-2 Sampling Ratio of Bottom Materials

Age	Classification	Sampling number	Ratio
Quarter-nary	Brown clay	63	47.0
	Siliceous clay	38	28.4
	Calc-siliceous clay	13	9.7
	Silic-calcareous clay	11	8.2
	Calcareous clay	2	1.5
	Calc-siliceous woods	2	1.5
	Silic calcareous woods	2	1.5
	Calcareous woods	2	1.5
Former	Siliceous woods	1	0.7

Calcareous sediments are scattered over the surveyed area, and the sampling ratio indicates a high value of 23.9%. Calcareous sediments are observed between 4,600 - 5,200m in water depth and a little frequently in the southern part of the surveyed area. Seamounts and sea knolls lie in these part.

## 2 Properties

Fig. 3-3-2 shows major microscope pictures of each bottom material. Properties of bottom materials are generally described in this section.

### (a) Brown clay and siliceous clay

The main component minerals of brown clay and siliceous clay are clay minerals, siliceous creature shells and a small amount of micronodules, pyroclastic materials, ichthyolith, zeolites, etc. Siliceous creature shells contains mainly radiolaria shells and diatomaceous shells. The content of the siliceous creature shells are between 5 - 15% in almost all the samples. Characteristically, bottom materials in the surveyed area contain large amount of micro-nodules indicating several %. Therefore, most bottom materials are coarse.

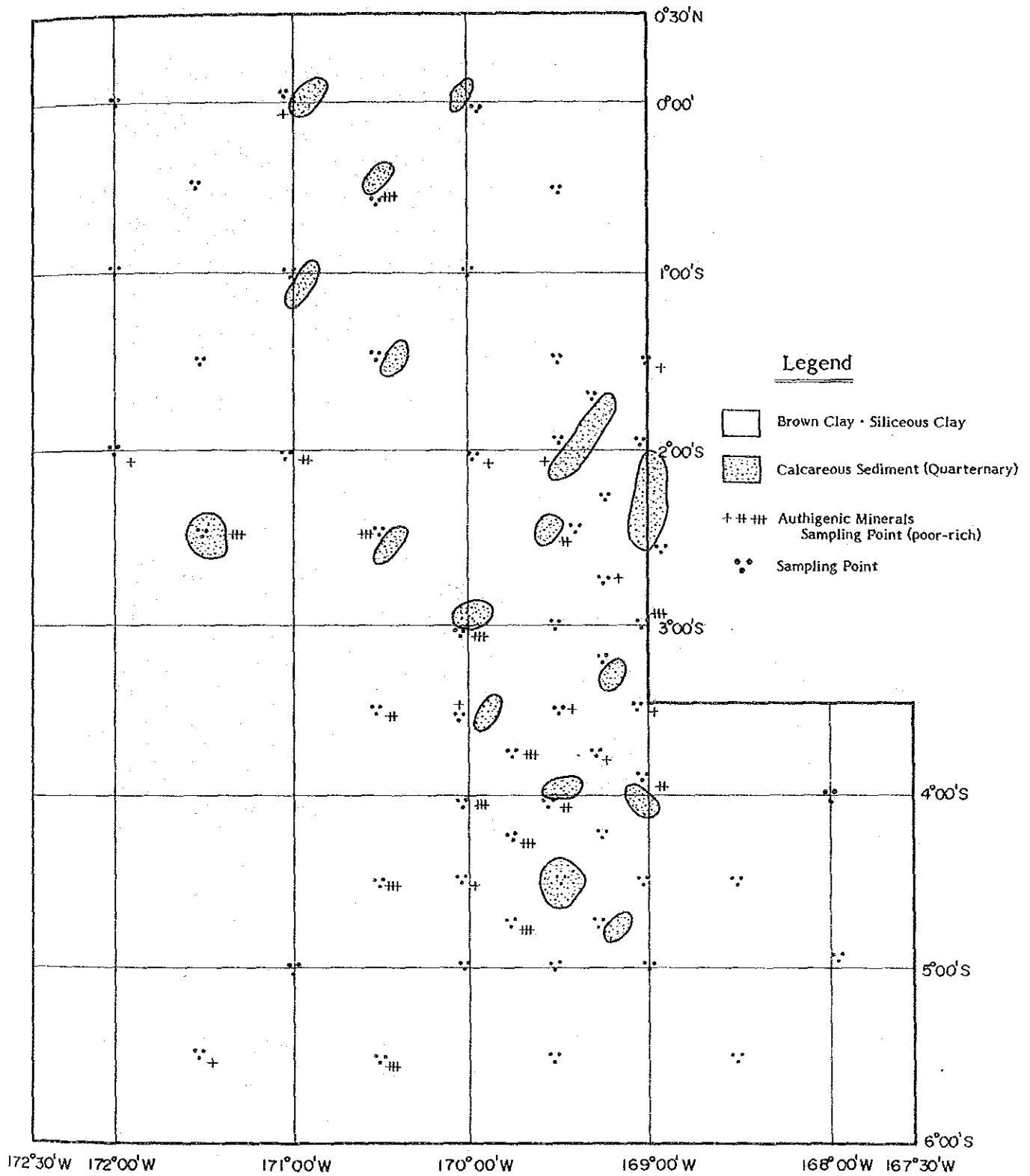
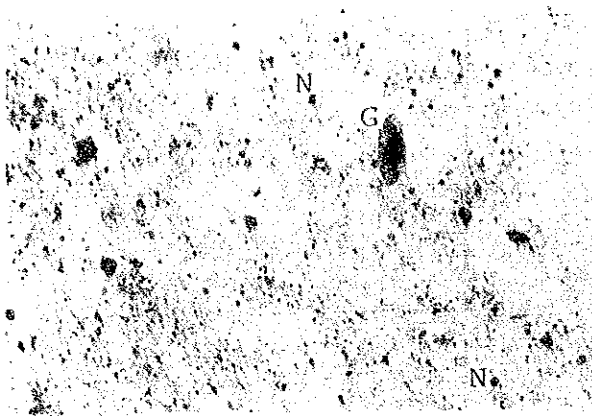
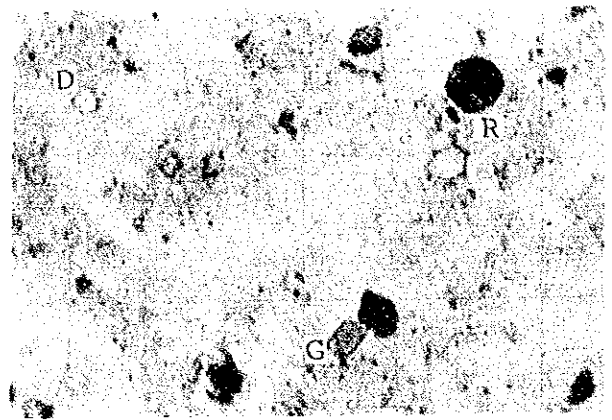


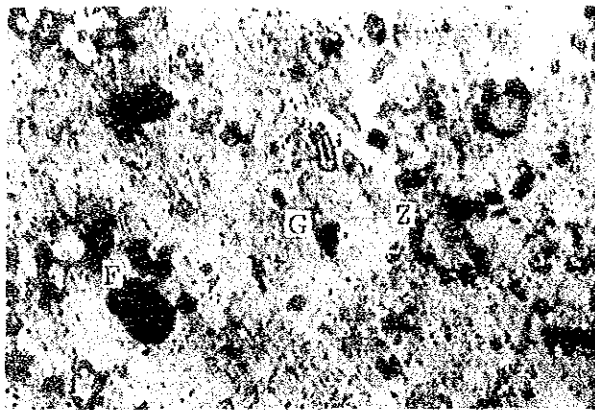
Fig. 3-3-1 Distribution of Bottom Materials



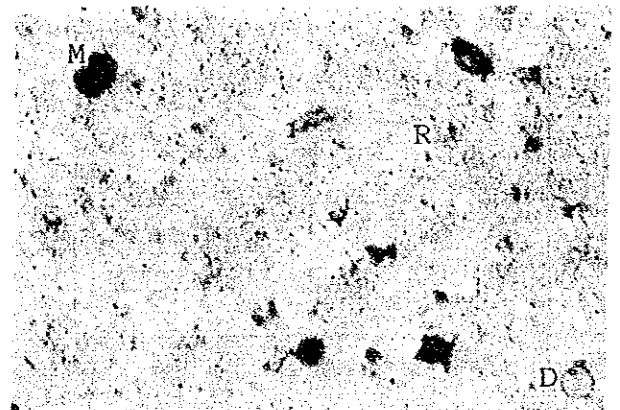
Brown clay (87S0471FG01)



Siliceous clay (87S0172FG04)



Calc Siliceous clay (87S0569FG01)



Silic-calcareous clay (87S0271FG04)

Legend

R: Radiolaria    D: Diatom    F: Foraminifera fragment    Z: Zeolite  
 M: Mud fragment    N: Micro-nodule    G: Volcanic glass

Fig. 3-3-2 Smear Slide photos of Bottom Sediments



(b) Calcareous sediments

Calcareous sediments are classified according to the quantitative ratio of calcareous creature shells and siliceous creature shells. In the surveyed area, calcareous-siliceous clay, siliceous-calcareous clay, calcareous clay, calcareous-siliceous ooze, siliceous-calcareous ooze and calcareous ooze are observed. Mainly, all of them consist of foraminifera debris and contain a small amount of micro-nodules, pyroclastic materials, ichthyolith, zeolites, etc. The bottom materials sampled on the seamounts, in the survey of cobalt crusts, are all coarse calcareous ooze.

(c) Siliceous ooze

Siliceous ooze consists of radiolaria and a large amount of micro-nodules. Siliceous ooze is recognized only one sampling point in the surveyed area. This point is the deep-set one in the surveyed area and the depth is approximately 6,265m.

3) Composing Minerals of Bottom Materials

Samples of the sea bottom materials by spade corer (SC) were taken from 6 points of the different depth of cored samples, and were examined by X-ray diffraction analysis to study mineral compositions. Tab. 3-3-3 and Fig. 3-3-3 show the results of analysis. Quartz, plagioclase, gypsum and clay materials are detected. Clay materials are illite, chlorite and montmorillonite. Halite is contained generally. It is observed that gypsum exists in the upper part of SC06 and SC02, and chlorite disappears at more than 40cm in depth of SC06. It makes no difference between the north part and the south part of the surveyed area (SC06 is sampled in the northern part, while SC02 is sampled in the southern part of the surveyed area).

4) Chemical Composition of Bottom Materials

Samples of the sea bottom material by spade corer (SC) were taken every 10cm from the surface layer, and were examined by chemical analysis. The results of the analysis are shown in Tab. 3-3-4. The following are proved by this analysis.

1. To compare with the upper layer and the lower layer, upper bottom materials have higher contents of  $Fe_2O_3$ , FeO,  $Na_2O$  and Ig-loss. On the other hand, lower bottom materials have a higher contents of  $SiO_2$ , BaO, MnO, etc. The contents

Table 3-3-3 Results of X-ray Diffraction Analysis of Bottom Materials

Sample No.	Minerals	Q	Pl	Mont	Il	Chl	Gyp	Ha
87S0270SC06	0 cm (Brown Clay)	±	±	±	±	±	±	±
"	10 cm (Siliceous Clay)	+	±	±	±	±	+	±
"	20 cm ( " )	+	±	±	±	±		±
"	30 cm (Siliceous ooze)	±	±	±	±	±		+
"	40 cm ( " )	±	±	±			±	+
"	50 cm ( " )	±	±	±				±
87S0668SC02	0 cm (Brown Clay)	±	±	±	±	±		±
"	10 cm (Siliceous Clay)	+	±	±	±	±	±	+
"	20 cm ( " )	+	±	±	±	±	±	±
"	30 cm ( " )	+	±	±	±	±	±	+
"	40 cm ( " )	±	±	±	±	±		±
"	50 cm (Brown Clay)	±	±	±	±	±		±

Legend: ++, +, ±, indicate intensity of diffraction peaks, (+: moderate, +: weak, ±: very weak)  
 Q : Quartz, Pl: Plagioclase, Mont: Montmorillonite  
 Il: Illite, Chl: Chlorite, Gyp: Gypsum, Ha: Halite

of MgO, B, Zn, Y, Co, As and Sr are almost constant and make no difference between the upper layer and the lower layer.

- The components such as MgO, B, Zn, Y, Co, As, and Sr indicate a different content between the upper layer and the lower layer; however, the content of each material has difference between the north and the south area.
- In comparison with the south area (SC02), the north area (SC06) has a higher contents of SiO<sub>2</sub>, Ig-loss, Ni, Cu, etc, while the south area has a higher contents of TiO<sub>2</sub>, Al<sub>2</sub>O<sub>3</sub>, Fe<sub>2</sub>O<sub>3</sub>, MgO, CaO, K<sub>2</sub>O, V and Sr. The contents of B, Zn, As, Co, etc. are almost equal both in the north and the south area.
- To compare with bottom materials of DOMES site-B\*<sup>1</sup>, bottom materials in this area have higher contents of MnO, MgO, Ig-loss, etc. On the other hand, bottom materials in this surveyed area have a lower contents of CaO, BaO, K<sub>2</sub>O, P<sub>2</sub>O<sub>5</sub>, B, etc.

\*1 SiO<sub>2</sub> 51.5%, TiO<sub>2</sub> 0.59%, Al<sub>2</sub>O<sub>3</sub> 12.5%, Fe<sub>2</sub>O<sub>3</sub> 5.4%, MnO 0.53%, MgO 3.0%, CaO 1.5%, Na<sub>2</sub>O 5.7%, K<sub>2</sub>O 3.3%, P<sub>2</sub>O<sub>5</sub> 0.51%, B 0.17%, Ig-loss 11.2%, (Bischoff, J.L et.al., 1979)

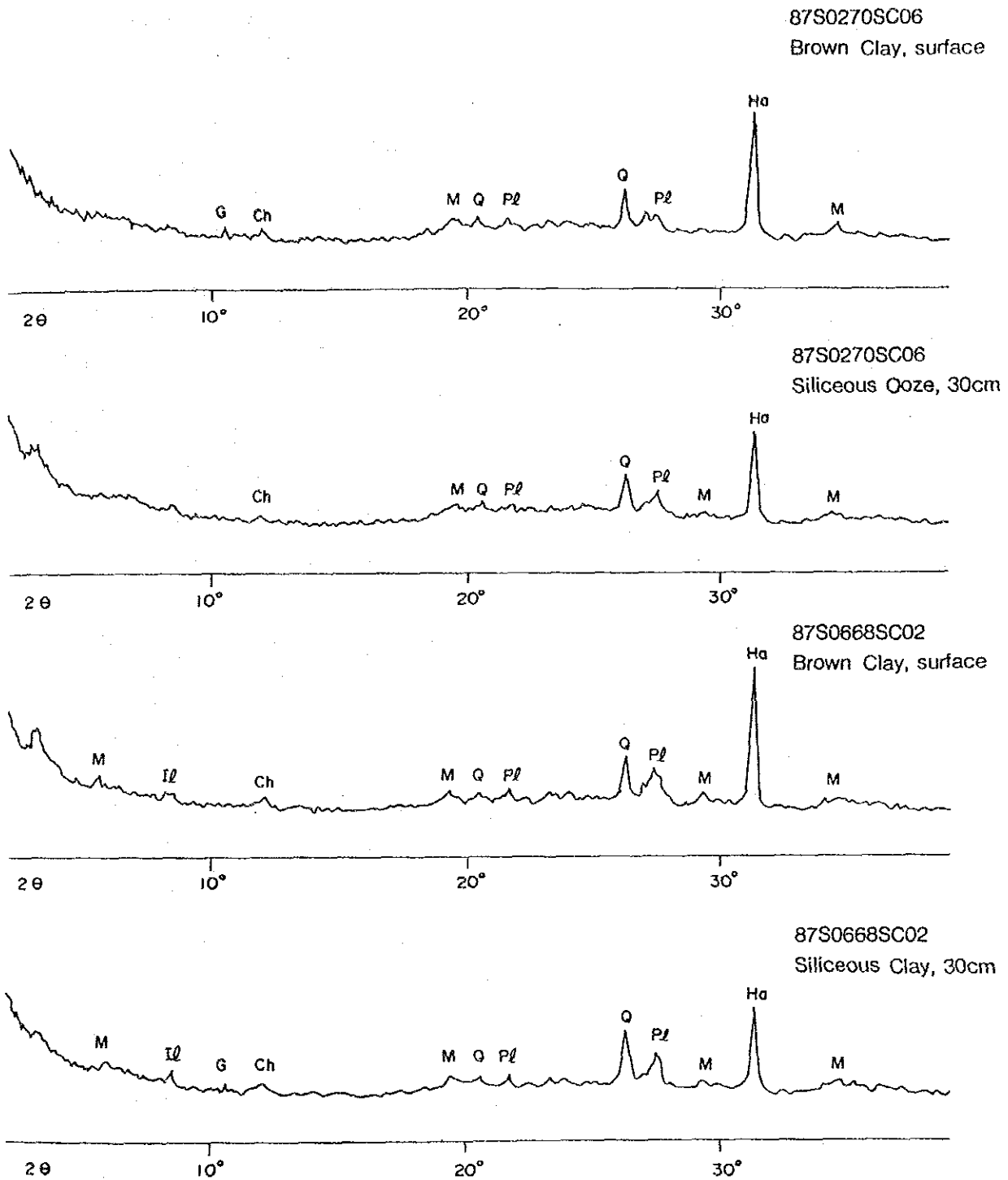


Fig. 3-3-3 Typical X-ray Diffraction Patterns of Bottom Sediments

Table 3-3-4 Chemical Composition of Bottom Materials

(%)

No.	Sample No.	Components and Values													
		SiO <sub>2</sub>	TiO <sub>2</sub>	Al <sub>2</sub> O <sub>3</sub>	Fe <sub>2</sub> O <sub>3</sub>	FeO	MnO	MgO	CaO	BaO	Na <sub>2</sub> O	K <sub>2</sub> O	P <sub>2</sub> O <sub>5</sub>	Ig-loss	
1	87506685C0237502705C06	Surface	50.40	0.47	10.19	3.95	1.07	0.68	2.75	1.58	0.18	7.19	1.52	0.52	18.67
2		10 cm	51.67	0.52	10.71	4.59	0.84	0.68	2.69	1.76	0.19	6.33	1.65	0.52	16.88
3		20 cm	52.95	0.56	11.12	5.42	0.39	0.86	2.71	1.59	0.20	5.81	1.71	0.48	15.47
4		30 cm	53.18	0.56	11.33	5.93	0.36	0.92	2.71	1.48	0.19	5.83	1.71	0.42	15.34
5		40 cm	57.01	0.35	7.96	3.46	0.30	0.84	2.24	1.19	0.30	6.81	1.38	0.34	15.35
6		50 cm	59.69	0.34	7.81	3.32	0.32	1.25	2.11	1.14	0.34	5.97	1.30	0.35	16.10
7		Surface	47.23	0.93	11.77	6.38	0.84	0.86	3.35	2.30	0.17	6.44	1.78	0.44	16.47
8		10 cm	47.51	0.97	12.03	6.63	0.68	0.87	3.42	2.30	0.20	6.45	1.73	0.43	15.47
9		20 cm	48.17	1.07	12.58	7.46	0.88	0.89	3.53	2.30	0.21	5.96	1.95	0.43	14.31
10		30 cm	48.31	1.05	12.62	7.43	0.49	0.92	3.46	2.15	0.22	5.70	1.93	0.42	14.42
11		40 cm	47.61	1.08	12.75	7.72	0.42	0.95	3.59	2.15	0.22	5.83	1.90	0.42	14.27
12		50 cm	47.87	1.13	13.09	8.01	0.32	0.96	3.67	2.22	0.21	5.58	1.89	0.46	14.13
X		51.5	0.59	12.5	5.4	-	0.53	1.5	3.0	1.5	-	5.7	3.3	11.2	

(%)

No.	Sample No.	Components and Values												
		Pb	V	B	Zn	Y	Ni	Cu	Co	As	Sr	Mo	Total	
1	87506685C0237502705C06	Surface	0.006	0.003	0.006	0.015	0.008	0.012	0.024	0.010	0.001	0.021	< 0.001	99.28
2		10 cm	0.025	0.004	0.007	0.013	0.008	0.013	0.037	0.010	0.001	0.022	< 0.001	99.17
3		20 cm	0.005	0.004	0.006	0.015	0.008	0.020	0.044	0.011	0.001	0.023	< 0.001	99.41
4		30 cm	0.005	0.003	0.006	0.014	0.007	0.020	0.040	0.011	0.001	0.022	< 0.001	99.59
5		40 cm	0.013	0.003	0.006	0.012	0.006	0.025	0.046	0.008	0.001	0.022	< 0.001	97.67
6		50 cm	0.004	0.003	0.006	0.013	0.007	0.047	0.070	0.014	0.001	0.022	< 0.001	100.23
7		Surface	0.006	0.004	0.006	0.016	0.006	0.009	0.030	0.012	0.001	0.027	< 0.001	99.08
8		10 cm	0.007	0.005	0.006	0.014	0.006	0.009	0.029	0.012	0.001	0.027	< 0.001	99.81
9		20 cm	0.007	0.005	0.006	0.015	0.006	0.010	0.030	0.012	0.001	0.029	< 0.001	99.86
10		30 cm	0.007	0.005	0.006	0.016	0.006	0.010	0.030	0.013	0.001	0.027	< 0.001	99.24
11		40 cm	0.006	0.011	0.006	0.017	0.006	0.009	0.033	0.013	0.001	0.028	< 0.001	99.04
12		50 cm	0.007	0.010	0.006	0.015	0.006	0.010	0.032	0.012	0.001	0.027	< 0.001	99.67
X		-	-	0.17	-	-	-	-	-	-	-	-	-	

No. 1 - 12 : Results of this survey  
 X : DOMES Site-B (Bischoff J.L. et al., 1979)

5 The correlation coefficients of chemical components are shown in Tab. 3-3-5. MnO indicates positive correlation with BaO, Ni, Cu, Co, etc. and negative one with P<sub>2</sub>O<sub>5</sub>. Fe<sub>2</sub>O<sub>3</sub> indicates positive correlation with MgO, CaO, K<sub>2</sub>O, V, Zn, Sr, etc. and negative one with Na<sub>2</sub>O, Ig-loss Ni, Cu, etc. Ni indicates positive correlation with SiO<sub>2</sub>, MnO, BaO, Cu, etc. and negative one with TiO<sub>2</sub>, Fe<sub>2</sub>O<sub>3</sub>, MgO, CaO, K<sub>2</sub>O and Zn.

Table 3-3-5 Correlations among Chemical Components of Bottom Materials

	SiO2	TiO2	Al2O3	Fe2O3	FeO	MnO	MgO	CaO	BaO	Na2O	K2O	P2O5	LOI	Pb	V	B	Zn	Y	Ni	Cu	Co	As	Sr	Hg
SiO2	1.00	-0.87	-0.91	-0.84	-0.45	0.38	-0.94	-0.95	0.77	0.14	-0.87	-0.49	0.24	0.09	-0.56	0.05	-0.75	0.38	0.94	0.89	-0.24	-0.01	-0.77	-0.01
TiO2		1.00	0.91	0.98	0.09	0.85	0.98	0.94	-0.43	-0.48	0.91	0.12	-0.63	-0.25	0.73	-0.24	0.73	-0.67	-0.72	-0.62	0.51	0.09	0.95	0.00
Al2O3			1.00	0.95	0.18	-0.18	0.94	0.99	-0.71	-0.58	0.97	0.42	-0.49	-0.17	0.65	-0.08	0.77	-0.36	-0.82	-0.73	0.38	-0.90	0.78	-0.00
Fe2O3				1.00	-0.01	0.86	0.96	0.99	-0.47	-0.69	0.95	0.15	-0.70	-0.26	0.75	-0.23	0.74	-0.59	-0.70	-0.59	0.49	-0.00	0.91	-0.00
FeO					1.00	-0.84	0.21	0.38	-0.38	0.58	0.19	0.63	0.61	0.24	-0.26	0.31	0.18	0.25	-0.49	-0.59	-0.16	0.00	0.07	-0.00
MnO						1.00	-0.18	-0.11	0.83	-0.56	-0.15	-0.71	-0.46	-0.54	0.11	-0.45	-0.02	-0.36	0.65	0.69	0.71	0.03	0.17	0.00
MgO							1.00	0.96	-0.57	-0.38	0.92	0.27	-0.51	-0.21	0.71	-0.19	0.77	-0.57	-0.82	-0.74	0.42	-0.00	0.90	-0.00
CaO								1.00	-0.61	-0.28	0.87	0.31	-0.49	-0.09	0.58	-0.06	0.69	-0.53	-0.82	-0.74	0.49	0.00	0.90	0.00
BaO									1.00	-0.05	-0.63	-0.80	-0.17	-0.07	-0.14	-0.18	-0.53	-0.17	0.83	0.83	0.12	0.00	-0.26	0.00
Na2O										1.00	0.33	0.59	0.14	0.62	-0.08	0.76	-0.42	-0.79	-0.68	0.36	-0.00	0.82	-0.00	0.00
K2O											1.00	0.45	0.39	0.97	0.48	0.30	0.59	-0.57	-0.59	-0.19	0.00	-0.00	0.00	0.00
P2O5												1.00	0.22	-0.60	0.31	-0.26	0.89	0.15	-0.31	-0.38	0.00	-0.07	0.00	0.00
LOI													1.00	-0.12	0.92	0.47	0.28	-0.13	-0.05	-0.53	0.00	-0.27	0.00	0.00
Pb														1.00	-0.12	0.58	-0.46	-0.44	-0.31	0.39	0.00	0.65	0.00	0.00
V															1.00	-0.35	0.47	-0.09	-0.00	-0.23	0.01	-0.29	0.01	
B																1.00	-0.26	-0.60	-0.56	0.52	0.00	0.65	-0.00	
Zn																	1.00	0.26	0.20	-0.32	0.00	-0.76	0.00	
Y																		1.00	0.97	0.10	-0.00	-0.59	-0.00	
Ni																			1.00	0.16	-0.00	-0.49	-0.00	
Cu																				1.00	0.00	0.54	0.00	
Co																					1.00	0.00	0.00	
As																						1.00	0.00	
Sr																							1.00	0.00
Hg																								1.00

5) Authigenic Minerals in Bottom Materials

With a view to analyzing the mineral components of authigenic minerals, the powder X-ray diffraction was carried out. The results are shown in Tab. 3-3-6 and Fig. 3-3-4. Quartz, montmorillonite and harmotome are detected and the diffraction indicates a high peak at harmotome.

Table 3-3-6 Result of X-ray Diffraction Analysis of Authigenic Minerals

Sample No.	Minerals	Qtz	Mont	Har
87S0570FG10		±	±	++
87S0570FG12		±	±	++

Legend : ++, +, ± indicate intensity of diffraction peaks, ( ++ : moderate, + : weak, ± : very weak)

Qtz : Quartz, Mont : Montmorillonite, Har : Harmotome

6) CCD (Carbonate Compensation Depth)

Maximum water depth in which carbonate minerals are not recognized through observation by microscope; calcium carbonate compensation depth (CCD) increases gradually from northern part to southern part in the surveyed area. CCD is approximately 5,200m in the northern part of 3° 00' S and 5,300m in the southern part of 3° 00' S.

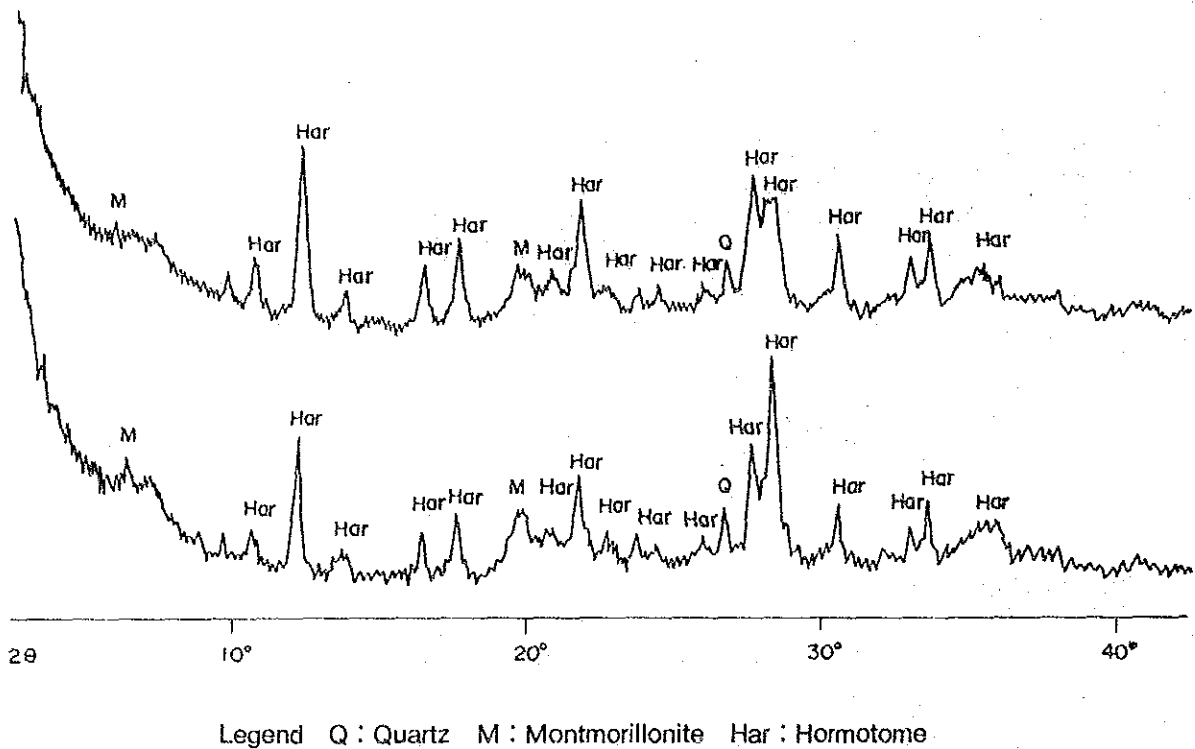


Fig. 3-3-4 Typical X-ray Diffraction Patterns of Authigenic Minerals

7) Identification of Microfossils in Bottom Materials

Through identification of fossils (Radiolaria, Foraminifera) in the bottom materials sampled by spade corer, sedimentary environment were examined.

Two samples were selected, one was in the northern part of the surveyed area and the other in the southern part. The sample numbers, sampling positions, water depth, and types of bottom sediments are as follows;

Sample No.	Sample Position	Sea depth	Type
87S0270SC06	00° 59.06' S, 169° 59.78' W	5,371m	Brown clay Siliceous clay Siliceous ooze
87S0668SC02	04° 58.99' S, 168° 01.08' W	5,340m	Brown clay Siliceous clay

(1) Radiolaria

1 Analysis method

Samples of 100cc was selected on board from 2 samples collected by a spade

corer at each of: the surface, 5cm, 10cm, 20cm, 30cm, and 40cm. In the laboratory samples of 20cc were taken, and were washed with water on a screen with a opening diameter of 62 $\mu$ m to concentrate the Radiolarias. The samples cleaned by HCl, H<sub>2</sub>O<sub>3</sub>, were further washed on a screen of the same diameter. Radiolarian occurrence list were made by observing and identifying with an optical microscope the dried samples packed into slide glass.

2 Occurrence of fossils (Tab. 3-3-7, Fig. 3-3-5)

(a) 87S0270SC06

The surface:

Many fossils as well as many different species were found in a good state of preservation. They included re-heaped (the surface of the frame was etched slightly) radiolaria less than 1%.

10cm: Many fossils as well as many different species were found in a good state of preservation. They included re-heaped radiolaria approximately 5%.

20cm: Many fossils as well as many different species were found in a good state of preservation. They included re-heaped radiolaria approximately 10%.

30cm: Many fossils as well as many different species were found in a good state of preservation. They included un-etched ones approximately 5%.

40cm: Many fossils as well as many different species were found in a good state of preservation. They consisted of only etched ones.

50cm: Many fossils as well as many different species were found in a good state of preservation. They consisted of only etched ones.

(b) 87S0668SC02

The surface:

Many fossils as well as many different species were found in a good state of preservation.

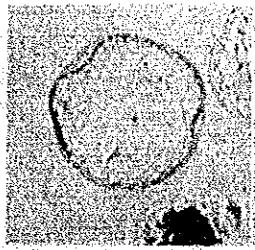
10cm: Many fossils as well as many different species were found in a good state of preservation.

20cm: Many fossils as well as many different species in a good state of preservation were found with a small amount of radiolaria with frame melt.

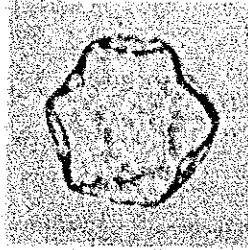
Table 3-3-7 List of Radiolarian Fossiles

Species \ Sample	8750270SC06					8750668SC02						
	Surface	10cm	20cm	30cm	40cm	50cm	Surface	10cm	20cm	30cm	40cm	50cm
Acrosphaera flammabunda (Haeckel)	X	X	X				X	X	X	X	X	X
A. lappacea (Haeckel)	X	X	X	X	X	X	X	X	X	X	X	X
A. murrayana (Haeckel)	X	X	X	X	X	X	X	X	X	X	X	X
A. spinosa Haeckel	X	X	X				X	X	X	X	X	X
Buccinosphaera invaginata Haeckel	X	X	X				X	X	X	X	X	X
Collosphaera huxleyi Muller	X	X	X				X	X	X	X	X	X
C. tuberosa Haeckel	X	X	X				X	X	X	X	X	X
Otosphaera polymorpha Haeckel	X	X	X				X	X	X	X	X	X
Siphonosphaera socialis Haeckel	X	X	X				X	X	X	X	X	X
Solenosphaera omnitubus Riedel and Sanfilippo				X	X	X						
Acanthosphaera capillaris Haeckel	X	X	X	X	X	X	X	X	X	X	X	X
Actinomma archadophorum Haeckel	X	X	X				X	X	X	X	X	X
A. spp.	X	X	X	X	X	X	X	X	X	X	X	X
Actinosphaera capillacea (Haeckel)	X	X	X				X	X	X	X	X	X
Amphisphaera cf. palliatum (Haeckel)	X	X	X				X	X	X	X	X	X
Axopium angelinum (Campbell and Clark)				X	X	X						
Bruppactrus spp.	X	X	X	X	X	X	X	X	X	X	X	X
Hexacantium spp.	X	X	X	X	X	X	X	X	X	X	X	X
Hexacantium spp.	X	X	X	X	X	X	X	X	X	X	X	X
Saturunalis circulae Haeckel	X	X	X	X	X	X	X	X	X	X	X	X
Stylatractus melpomene (Haeckel)	X	X	X	X	X	X	X	X	X	X	X	X
S. cf. neptunus Haeckel	X	X	X				X	X	X	X	X	X
Thecosphaera radianus Holland and Enjumeit	X	X	X				X	X	X	X	X	X
Xiphatractus sp.	X	X	X				X	X	X	X	X	X
Ommatarius tetrathalamus tetrathalamus (Haeckel)	X	X	X	X	X	X	X	X	X	X	X	X
Ü. penultimus				X	X	X						
Heliodiscus asteriscus Haeckel	X	X	X	X	X	X	X	X	X	X	X	X
Amphirhopalum ypsilon Haeckel	X	X	X	X			X	X	X	X	X	X
Eucitonia elegans Ehrenberg	X	X	X				X	X	X	X	X	X
E. frucata Ehrenberg	X	X	X	X	X	X	X	X	X	X	X	X
Dictyocoryne profunda Ehrenberg	X	X	X	X	X	X	X	X	X	X	X	X
D. truncatum (Ehrenberg)	X	X	X	X	X	X	X	X	X	X	X	X
Spongaster tetras tetras Ehrenberg	X	X	X	X	X	X	X	X	X	X	X	X
S. pentas Riedel and Sanfilippo	X	X	X	X	X	X	X	X	X	X	X	X
Spongodiscus spp.	X	X	X	X	X	X	X	X	X	X	X	X
Stylodictia spp.	X	X	X	X			X	X	X	X	X	X
Xiphospira spp.	X	X	X				X	X	X	X	X	X
Larcospira quadrangura Haeckel	X	X	X	X	X	X	X	X	X	X	X	X
Tetrapyle octacantha Muller	X	X	X	X	X	X	X	X	X	X	X	X
Clathromitra pentacantha Haeckel	X	X	X				X	X	X	X	X	X
Clathrocanium reginae Haeckel	X	X	X				X	X	X	X	X	X
Pseudodictyophimus glacilipes (Bailey)	X	X	X				X	X	X	X	X	X
Lampromitra butschlii (Haeckel)	X	X	X				X	X	X	X	X	X
Botryocorytis scutum (Harting)	X	X	X	X			X	X	X	X	X	X
Carpocanium spp.	X	X	X	X			X	X	X	X	X	X
Eucecryphalus elizabethae (Haeckel)	X	X	X				X	X	X	X	X	X
Cyclampterium neatum Sanfilippo and Riedel					X	X						
Dictyophimus infabricatus Nigrini	X	X	X	X	X	X	X	X	X	X	X	X
Eucyrtidium acuminatum Ehrenberg	X	X	X	X	X	X	X	X	X	X	X	X
E. anomalum (Haeckel)	X	X	X	X	X	X	X	X	X	X	X	X
E. dictyopodium (Haeckel)	X	X	X	X			X	X	X	X	X	X
Lipmanella bombus (Haeckel)	X	X	X				X	X	X	X	X	X
L. virchowii (Haeckel)	X	X	X	X			X	X	X	X	X	X
Lithopera bacca Ehrenberg	X	X	X	X	X	X	X	X	X	X	X	X
Lychnodictyum audax Riedel					X							
Pterocanium charibdeum (Muller)	X	X	X				X	X	X	X	X	X
P. praetextum (Ehrenberg)	X	X	X	X			X	X	X	X	X	X
P. prismatium Riedel				X	X	X						
P. trilobium (Haeckel)	X	X	X				X	X	X	X	X	X
Stichocorys peregrina (Riedel)				X	X	X						
Anthocyrtidium ophirensis (Ehrenberg)	X	X	X	X	X	X	X	X	X	X	X	X
A. zanguebaricum (Ehrenberg)	X	X	X	X	X	X	X	X	X	X	X	X
Lamprocycelas maritima Haeckel	X	X	X	X	X	X	X	X	X	X	X	X
Lamprocycelis gamphonycha (Jorgensen)	X	X	X				X	X	X	X	X	X
L. haysi Kling	X	X	X	X			X	X	X	X	X	X
L. neoheteroporos Kling												
L. sp. cf. L. heteroporos (Hays)				X	X	X						
Pterocorys hertwigii (Haeckel)	X	X	X	X			X	X	X	X	X	X
P. macroceras (Popofsky)	X	X	X				X	X	X	X	X	X
P. zancleus (Muller)	X	X	X	X	X	X	X	X	X	X	X	X
Theocorythium trachelium (Ehrenberg)	X	X	X	X			X	X	X	X	X	X
Botryostrobos aquilonaris (Bailey)	X	X	X	X	X	X	X	X	X	X	X	X
B. auritus (Ehrenberg)	X	X	X	X	X	X	X	X	X	X	X	X
Phrmstichoartus corbula (Harting)	X	X	X	X	X	X	X	X	X	X	X	X
P. doliola (Riedel and Sanfilippo)				X	X	X						
Spirocorytis scalaris Haeckel	X	X	X	X	X	X	X	X	X	X	X	X
S. subscalaris Nigrini	X	X	X	X	X	X	X	X	X	X	X	X
Acanthodesmia vuniculata (Muller)	X	X	X				X	X	X	X	X	X
Liriospyris reticulata (Ehrenberg)	X	X	X				X	X	X	X	X	X
Nephrospyris renilla Haeckel	X	X	X				X	X	X	X	X	X
Zigocircus capulosus Popofsky	X	X	X				X	X	X	X	X	X

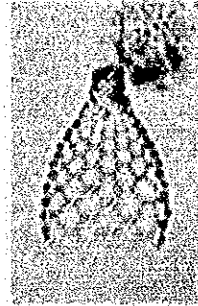




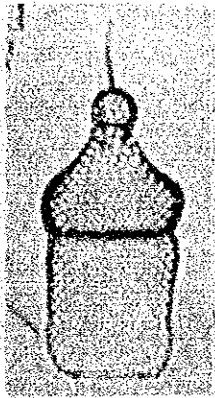
1



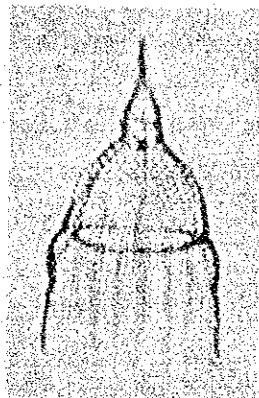
2



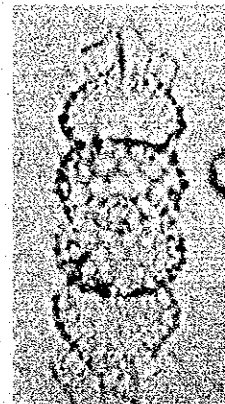
3



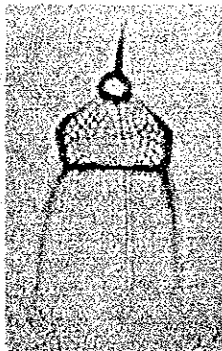
4



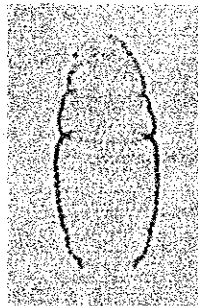
5



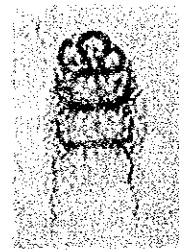
6



7



8

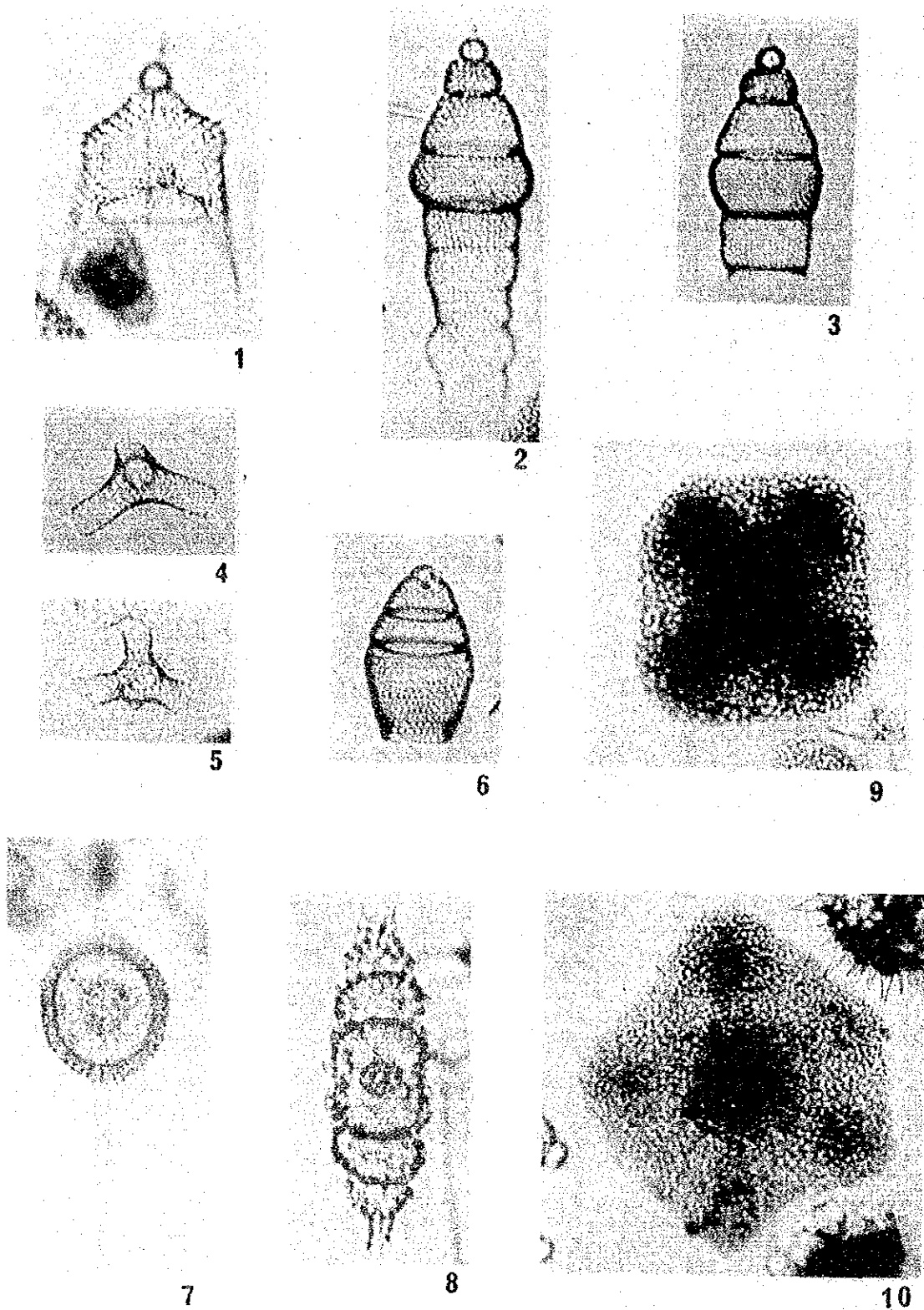


9

- 1 *Buccinosphaera invaginata* × 200
- 2 *Collosphaera tuberosa* × 200
- 3 *Lamplocyrtis haysi* × 200
- 4 *Theocorythium tracherlium* × 200

- 5 *Pterocorys hertwigii* × 200
- 6 *Ommatartus tetratalamus tetrathalamus* × 200
- 7 *Pterocanium praetextum* × 200
- 8 *Phormostichoartus corbula* × 200
- 9 *Botryocyrtis scutum* × 200

Fig. 3-3-5 Species of the Typical Radiolarian Fossils (1)



- 1 *Pterocanium prismatium* × 200
- 2, 3 *Stichocorys peregrina* × 200
- 4, 5 *Solenosphaera omunitubus* × 200
- 6 *Phormostichoartus doliola* × 200

- 7 *Axoplunum angelinum* × 200
- 8 *Ommatartus penultimus* × 200
- 9 *Spongaster tetras tetras* × 200
- 10 *Spongaster pentas* × 200

Fig. 3-3-5 Species of the Typical Radiolarian Fossils (2)

30cm: Many fossils as well as many different species in a good state of preservation were found with a small amount of radiolaria with frame melt.

40cm: Many fossils as well as many different species in a good state of preservation were found with a small amount of radiolaria with frame melt.

50cm: Many fossils as well as many different species in a good state of preservation were found with a small amount of radiolaria with frame melt.

3 Un-etched radiolaria in the samples between the surface and 30cm level of "87S0270SC06" and radiolaria in all the samples of "87S0668SC06" belong to present period. They contain *Collosphaera Tuberosa* Haeckel, *Amphirhopalum ypsilon* Haeckel which appeared in the later part of Quarternary period (about 400,000 years ago) and *Buccinosphaera invaginata* Haeckel which appeared in about 200,000 years ago except the sample of 30cm level in "87S0270SC06". The group of etched radiolaria in the samples of 30cm, 40cm and 50cm level in "87S0270SC06" contain *Pterocanium prismatium* Riedel, *Stichocorys peregrina* (Riedel), *Phormostichoartus dliola* (Riedel and Sanfilippo) and *Spongaster pentas* Riedel and Sanfilippo. While, they do not contain *S. berminghami* Campbell and Clark which is an ancestor type of *S. pentas*. They rarely contain *S. tetras* Ehrenberg which is a descendant type of *S. pentas*. This group correspond to the lower part of *Spongaster pentas* Zone (the lower Pliocene). According to these facts, in "87S0270SC06", the upper part of 20cm level is the sediments of younger than the upper Pleistocene (younger than those of 200,000 years ago), and the lower part of 30cm level is the sediments of the lower Pliocene (approximately 4 million years ago), and the existence of unconformity is presumed between 20cm and 30cm levels. The etched radiolaria contained in the samples above 20cm level are the same species as those in the samples below 30cm level, so that it is considered that those are re-heaped from the lower horizon. The un-etched radiolarias contained in the sample of 30cm level could be considered that those mingled were from the upper horizon, because the fossils are poor in number and the etched ones are the same composition as those in the lower level. The disturbance by creatures is considered as a reason for the mixture. The all part in "87S0668SC02" is the sediments of younger than the upper Pleistocene (200,000 years ago).

#### 4 Sedimentation speed

"87S0270SC06": the sedimentation speed above 20cm level is more than 1mm per thousand years supposing that the 20cm level is younger than 200,000 years ago. The faster sedimentation speed limit could not be determined. The sedimentation speed below 30cm level can not be calculated because the data of time are still unknown. "87S0668SC02": the sedimentation speed is more than 2.5mm per thousand years.

#### 5 Paleo-environment

All observed radiolaria are of species which generally live in the equatorial Pacific ocean. According to the present data concerning with species distribution, there is no significant difference between the radiolaria in "87S0270SC06" and those in "87S0668SC02". There is no established theory about the environment which makes the radiolaria melting. The significant melting is observed at the sedimentation speed of less than 1mm per thousand years, and almost all the radiolaria are melted at the sedimentation speed of less than 0.1mm per thousand years. A little melting is observed in the radiolaria in the levels of lower than 20cm, so that it is not recognized that the sedimentation speed of this horizon is more than 10mm per thousand years.

### (2) Foraminifera (cf. Tab. 3-3-8 and Fig. 3-3-6)

#### 1 Analysis method

The above mentioned two core-samples were taken on board by inserting a plastic tube (6cm in bore and 50cm in length) into the bottom materials' sample collected by spade corer. The plastic tube containing sea bottom materials were cut vertically by an electric buzz saw in the laboratory. The core contained was cut vertically into two portions by a knife. From one of the two portions obtained from the two cores were obtained the following six samples.

	Depth of sample
87S0270SC06	0 - 15 cm
	15 - 30 cm
	30 - 45 cm
87S0668SC02	0 - 14 cm
	14 - 28 cm
	28 - 42 cm

Table 3-3-8 List of Foraminifera Fossiles

CORE DEPTH (cm)	87S 0270 SC06			87S 0668 SC02		
	0-15	15-30	30-45	0-14	14-28	28-42
<i>Ammobaculites</i> SP.	3			2		2
<i>Alveolophragmium weisneri</i> (Parr)	6		3	7	1	1
A. SP.		3				
A. SP. indet.				1		1
<i>Bathysiphon</i> SP.	17	1	1		2	1
<i>Conostrochamina</i> SP.	2					
<i>Cribrestomoides</i> SPP.				6	1	
<i>Cystommina</i> SP.	4		1	4		
<i>Glomospira gordialis</i> (Jones & Parker)	12			7	2	8
<i>Haplophragmoides</i> SP.						2
<i>Recurvoides</i> SPP.	20		6	30	25	20
<i>Reophax nodulosus</i> Brady				1		
R. <i>pillulifer</i> Brady	2					
R. SPP.	7					11
R. SP. indet.	3			5	8	
<i>Trochammina</i> SP.	5			4	1	3

Each sample was hot-watered, muddied and washed on a screen of 200 mesh, then, all floating and bentic foraminifera remained on the screen were examined.

## 2 Results of analysis

### (a) Floating foraminifera community

Floating species were hardly observed in the analyzed samples.

### (b) Bentic foraminifera community

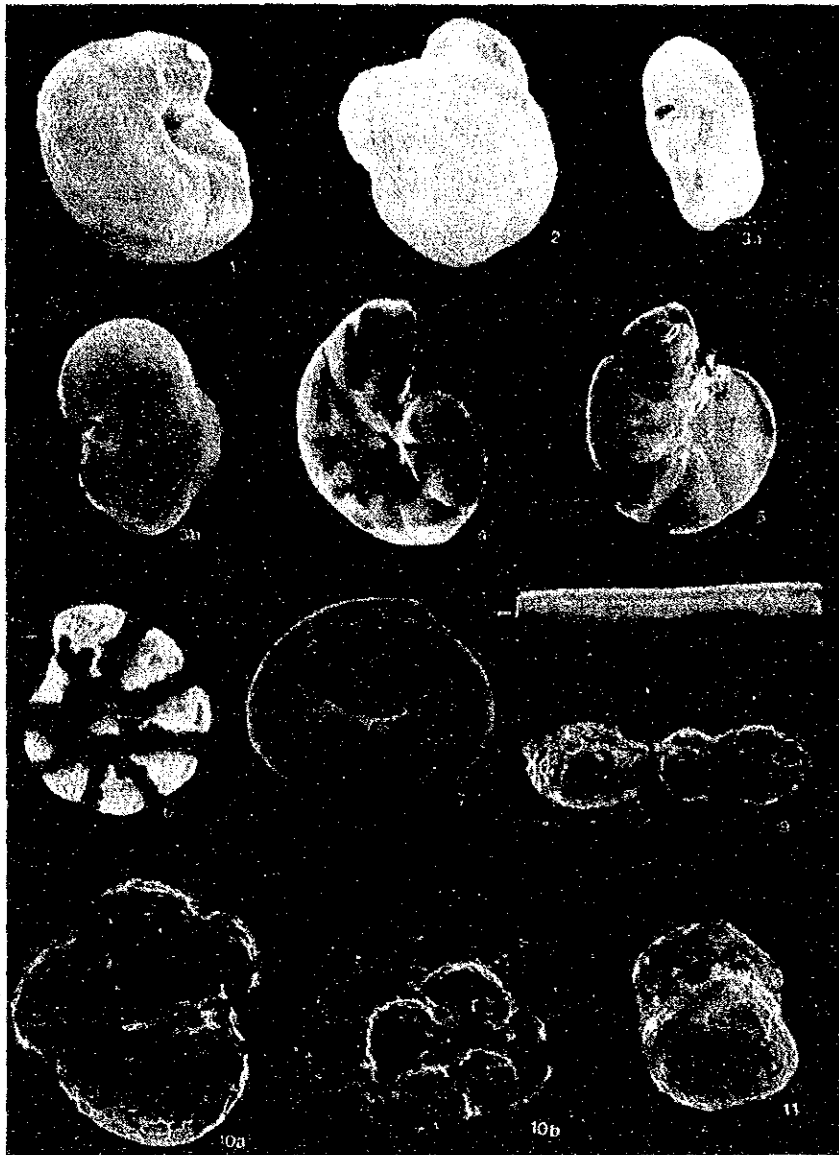
A few bentic foraminifera communities were relatively contained more than calcareous ones in all six samples. The contained main species are *Alveolophragmium weisneri*, *Glomospira gordialis*, *Recurvoides* SPP., *Haplophragmoides* SP., etc; however, they are barely observed.

## 3 Geological age

Nothing accurate was drawn about the age because there was no floating species contained.

#### 4 Paleo-environment

It was presumed that the sedimental environment was lower than CCD because *Recurvoides* SP. (a sandy species) accounted for 60% of whole and *Bathysiphon* SP., *Reophax* SP. (some species) were observed with that.



- |  |       |   |       |
|--|-------|---|-------|
| 1. <u>Conotrochamina</u> SP. ?                         | × 100 | 7. <u>Glomospira gordialis</u> (Jones & Parkar)         | × 175 |
| side view : 87S 0270 SC06 0-7cm                        |       | side view : 87S 0270 SC06 0-7cm                         |       |
| 2. <u>Recurvoides</u> SP.                              | × 75  | 8. <u>Bathysiphon</u> SP.                               | × 50  |
| side view : 87S 0270 SC06 0-7cm                        |       | side view : 87S 0270 SC06 0-7cm                         |       |
| 3a-b. <u>Cystamina</u> SP.                             | × 100 | 9. <u>Reophax</u> SP.                                   | × 75  |
| a. apertural view ; b. side view : 87S 0270 SC06 0-7cm | × 75  | side view : 87S 0270 SC06 7-15cm                        |       |
| 4. <u>Alveolophragmium</u> SP.                         | × 100 | 10a-b. <u>Trochammina</u> SP.                           | × 250 |
| side view : 87S 0270 SC06 0-7cm                        |       | a. ventral view ; b. dorsal view : 87S 0668 SC02 7-14cm |       |
| 5. <u>Alveolophragmium</u> wiesneri (Parr)             | × 75  | 11. <u>Recurvoides</u> SP.                              | × 100 |
| side view : 87S 0270 SC06 0-7cm                        |       | side view : 87S 0668 SC02 21-28cm                       |       |
| 6. <u>Alveolophragmium</u> SP.                         | × 100 |   |       |
| side view : 87S 0668 SC06 0-7cm                        |       |   |       |

Fig. 3-3-6 Species of the Typical Foraminifera Fossils

### 3-4 Research on Manganese Nodules by Means of MFES

#### 1) Factors Affecting on MFES

##### (1) Size of manganese nodules (weight coefficient)

By means of MFES, the sound pressure of three different frequencies such as NBS (30 kHz), PDR (12 kHz) and SBP (3.5 kHz), were measured individually and summed numerically to the compound sound pressure so as to estimate the abundance of manganese nodules on the deep ocean sea floor. Supposing a linear relation between the compound sound pressure and the abundance of manganese nodules  $V$  ( $\text{kg}/\text{m}^2$ ), a hypothetical formula listed below was given a priori. Later parameters  $a$  and  $b$  were determined based on the field data;

$$v = a \cdot Rt + b \dots \dots \dots (1)$$

According to the supposition by means of MFES, the compound sound pressure ( $Rt$ ) is in proportion to the covering ratio of bottom surface, regardless of the granular diameter of manganese nodules. Therefore, MFES detects the covering ratio of manganese nodules first based on the compound sound pressure which is reflected by the surface of manganese nodules and then the abundance of manganese nodules are calculated with weight coefficient given independently which means weight per unit covering surface of manganese nodules.  $22 \text{ kg}/\text{m}^2$ \*1 was the weight coefficient\*2 of manganese nodules adopted tentatively through the survey for immediate data analysis. The average of weight coefficient values in the surveyed area was calculated at  $24.6 \text{ kg}/\text{m}^2$  and close to the tentative value.

However, the values varied as shown in Fig. 3-4-1. So, the diameter obtained by MFES with the tentative value of weight coefficient could not be applied to the abundance of manganese nodules directly. therefore, the weight coefficient was needed to be adjusted in order to obtain more accurate abundance of manganese nodules by following formula.

$$\begin{aligned} &\text{The estimated abundance by MFES (kg/m}^2\text{)} \\ &= \text{Tentative abundance} \times \text{Weight coefficient}/22 \dots \dots \dots (2) \end{aligned}$$

---

\*1 Weight coefficient ( $\text{kg}/\text{m}^2$ ) =  
Recollected weight of manganese nodules ( $\text{kg}$ ) /  
(covering surface ratio x Grab-opening area ( $\text{m}^2$ ))  
= Abundance of manganese nodules ( $\text{kg}$ ) / Covering surface ratio

\*2 This was used to determine the parameter of the formula (1)



## (2) Topography and bottom materials

The relation between the estimated abundance (MFES value) of manganese nodules obtained by MFES observation and the abundance by sampling in the survey area is shown in Fig. 3-4-2-(1). As shown in the figure, the correlation coefficient indicates relatively a better value of 0.83. However, it is recognized that these data are divided into two groups on the abundance situation. In the group which shows the MFES value is higher, the data were mainly obtained at the plain and the stations are of type  $d_2$  and type  $ds$  composed of opaque layers in the upper part. Therefore, these data were recognized as so called Quasi-anomaly; sound pressure reflected by rock or hard bottom materials tends to be higher than its normal value. The relation between MFES value and abundance obtained by FG is shown in Fig. 3-4-2-(2) excluding the data of these Quasi-anomalies. On this figure, the correlation coefficient is the same value as that on Fig. 3-4-2-(2), but the variation of the data decreases. Therefore, the coefficient of gradient become close to "1" and the correlation coefficient improves. However, the data still varies a little. These data were obtained in the area where sea mounts and sea knolls of type  $d_1$  were distributed. In the sea mount and sea knoll, the Quasi-anomalies were observed sometimes, while the normal values could not be obtained because of the scattering wave and side-echo due to the intricate topography. It was considered that the reliability of the data was not sufficient. Therefore, the correlation was examined excluding the data of sea mounts and sea knolls. Fig. 3-4-2-(3) shows the correlation of the data which are obtained from the area covered with the transparent layer. The amount of data is not sufficient and the range is narrow, but the correlation coefficient is calculated at 0.93 and the coefficient of gradient is close to "1". The correlation is recognized good. As above mentioned, it is necessary to take into consideration the following.

- o Specially at the area where the opaque layer covers a great portion of the whole sea area, as this surveyed area, it is highly probable that Quasi-anomalies are observed in the station which is in the plain and type  $d_2$ ,  $ds$ .
- o The reliability of the data is not sufficient on the sea mounts and sea knolls.

## 2) Embedded Manganese Nodules

Although it was already pointed out that the embedded manganese nodules were able to be detected by MFES, its reexamination was done again because a large amount

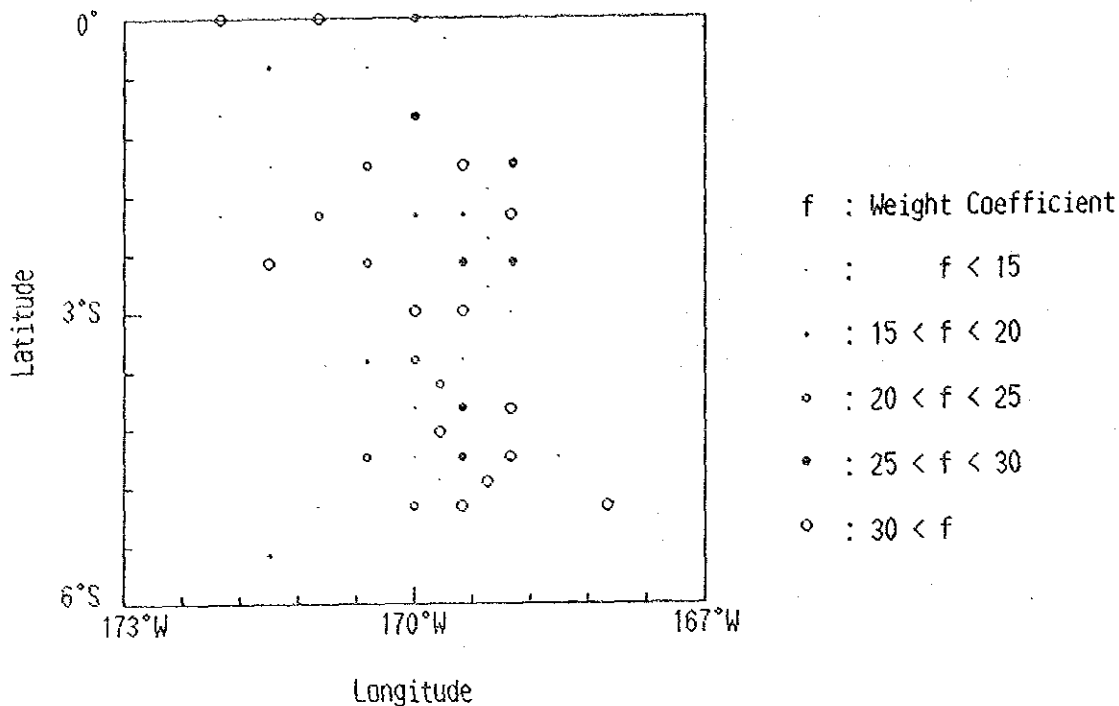
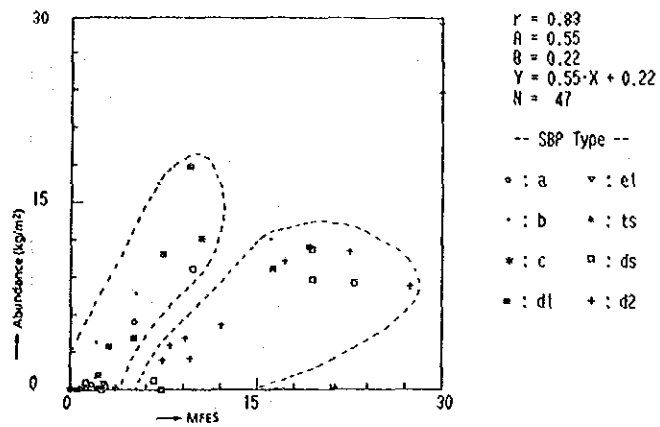


Fig. 3-4-1 Distribution of Weight Coefficient

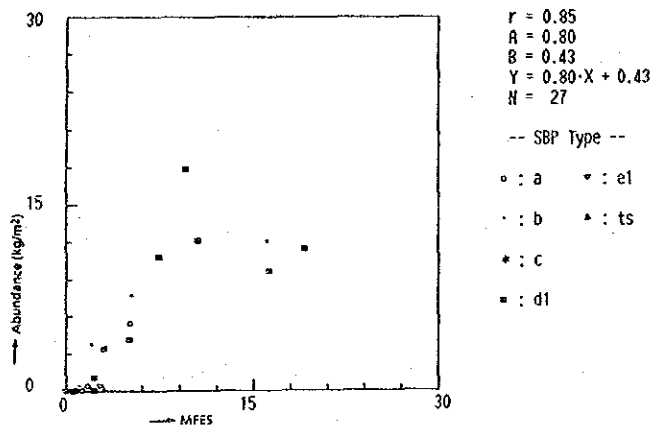
of embedded manganese nodules existed in the present surveyed area. The embedded manganese nodules are manganese nodules whose FGPOP are more than BTMPOP. In this case, the embedded manganese nodules which meet the following formula are considered as highly embedded ones.

$$(1 - \text{BTMPOP} / \text{FGPOP}) > 0.4$$

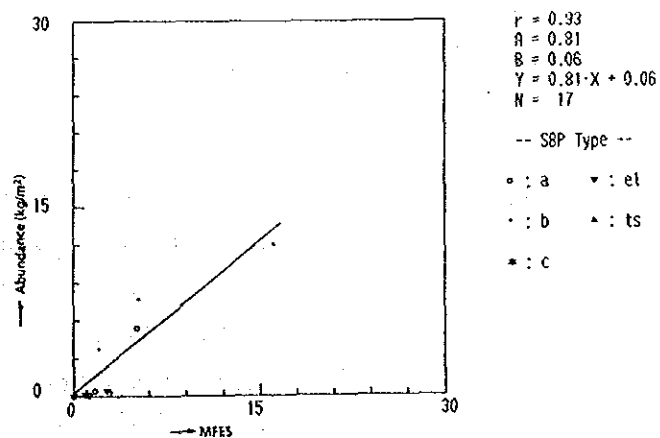
The distribution of embedded manganese nodules are shown in Fig. 3-4-3. When embedded manganese nodules are detected by MFES, MFES are measured higher than BTMPOP and close to FGPOP. This is shown in Fig. 3-4-4. Solid dots in the figure shows embedded manganese nodules of more than 0.4 in the embedded ratio, and open circle shows manganese nodules which are not embedded. probably. According to Fig. 3-4-4-(1), BTMPOP of embedded manganese nodules are extremely lower than MFES. It is recognized in Fig. 3-4-4-(2) that FGPOP are nearly the same as MFES and these correlation indicates 1:1. Therefore, embedded manganese nodules are sufficiently detected by means of MFES in the surveyed area. Fig. 3-4-4-(3) shows that embedded manganese nodules can be measured by MFES in the same as exposed type in the view of the comparison of abundance.



(1) Whole survey stations



(2) Excluding type d2 and ds



(3) Excluding type d2, ds and d1

Fig. 3-4-2 Relation Between MFES Intensity and Abundance of Manganese Nodules